TUBE WAVE GENERATION AT A LAYER BOUNDARY FOR AN INCIDENT COMPRESSIONAL PLANE WAVE

by

Chengbin Peng and M. Nafi Toksöz

Earth Resources Laboratory
Department of Earth, Atmospheric, and Planetary Sciences
Massachusetts Institute of Technology
Cambridge, MA 02139

ABSTRACT

An approximate theory for the scattering of an incident plane P wave into tube waves in a fluid-filled borehole drilled through two homogeneous half-spaces is proposed in this paper. This theory is in excellent agreement with the zero frequency formulation (White, 1983) for frequencies below hundreds of Hertz (in the range of conventional crosshole or VSP experiments) and finite difference simulation at high frequencies. At low frequency the excited tube wave is found to be independent of the borehole radius and shows stronger sensitivity to the formation shear velocity contrast across the layer boundary. The sensitivity towards the compressional velocity perturbation is opposite to that of the shear wave and density such that little tube wave can be generated if the compressional and shear velocities are both increased or decreased accordingly. Unlike the tube wave excited in the borehole when an incident plane wave hits a fracture, the reflected and transmitted tube waves generated at a layer boundary show opposite polarities.

INTRODUCTION

The problem of a plane wave incident at a fluid-filled borehole has been studied by White (1953) and Schoenberg (1986). White considered only the zero frequency limit. Schoenberg formulated the problem using exact theory, but invoked the low frequency approximation for numerical evaluations. Neither of these studies showed that a tube wave would be generated inside the borehole.

There is a physical explanation for the absence of tube waves in a homogeneous formation at long wavelengths. The tube wave would be generated if the pressure increments inside the borehole added constructively along the borehole axis. This does

not happen since the tube wave phase velocity is lower than the apparent vertical velocity of the incident wave. In cross-hole field experiments, one generally observes tube waves being generated in the receiver borehole. This commonly happens when the incident body waves hit a "borehole washout." It also happens at some formation boundaries.

In this paper we investigate the case of a plane P wave incident at a borehole drilled through two homogeneous half-spaces. The borehole axis is perpendicular to the interface between the two formations. We investigate how the formation properties, angle of incidence and frequency affect tube wave generation.

THEORETICAL FORMULATION

The model we consider is a borehole perpendicular to the interface between two homogeneous half-spaces. The incident wave is a plane P wave. To deal with the discontinuity, we use sources along the interface and inside the borehole to satisfy the boundary conditions.

We formulate the problem for each half-space (referred to as medium #1 and medium #2) separately, for using the low frequency approximation. The models of White (1953) and Schoenberg (1986) are illustrated schematically in Figure 1. For White's approach, the deformation of the borehole can be calculated by Timoshenko's theory (Timoshenko and Goodier, 1951) in static elasticity. The pressure set up across a differential distance dz along the borehole with medium #1 can be expressed as

$$dP_I = \rho_f C_T^I \omega S(\omega)[A^I_{P_\downarrow}\, e^{ik_{zp1}z} + A^I_{P_\downarrow P_\uparrow}\, e^{-ik_{zp1}z} + A^I_{P_\downarrow S_\uparrow}\, e^{-ik_{zs1}z}]dz, \qquad (1)$$

assuming a P-wave incidenvr from medium #1, where $A^I_{P_\downarrow}$ represents the contribution from the incident P wave; $A^I_{P_\downarrow P_\uparrow}$ represents the contribution from the reflected P wave, and $A^I_{P_\downarrow S_\uparrow}$ is the reflected S wave; ρ_f is the fluid density, C_T^I is the zero-frequency tube wave velocity in a borehole with medium #1, and $S(\omega)$ is the amplitude of incident P wave at frequency ω. Details of derivation can be found in the appendix A.

For the same reason, in the portion of the borehole with medium #2, the pressure set up by the transmitted P and S wave is

$$dP_{II} = \rho_f C_T^{II} \omega S(\omega)[A^{II}_{P_\downarrow P_\downarrow}\, e^{ik_{zp2}z} + A^{II}_{P_\downarrow S_\downarrow}\, e^{ik_{zs2}z}]dz. \qquad (2)$$

The total pressure at any point of the borehole will be the intergation of all the infinitesimal pressures along the borehole with appropriate phase delay. For a point in the borehole in medium #1, the pressure is

$$P(H<0,\omega) \;=\; \rho_f C_T^I \omega S(\omega)[B^I_{P_\downarrow}\, e^{ik_{zp1}H} + B^I_{P_\downarrow P_\uparrow}\, e^{-ik_{zp1}H} + B^I_{P_\downarrow S_\uparrow}\, e^{-ik_{zs1}H}]$$

$$+ \quad \rho_f C_T^I \omega S(\omega) B_{11}(A^I_{P_\downarrow}, A^I_{P_\downarrow P_\uparrow}, A^I_{P_\downarrow S_\uparrow})\, e^{-ik_{c1}H}$$
$$+ \quad \rho_f C_T^{II} \omega S(\omega) B_{12}(A^{II}_{P_\downarrow P_\downarrow}, A^{II}_{P_\downarrow S_\downarrow})\, e^{-ik_{c1}H}. \tag{3}$$

For a point in the borehole in medium #2, the pressure is

$$\begin{aligned} P(H>0,\omega) &= \rho_f C_T^{II} \omega S(\omega)[B^{II}_{P_\downarrow P_\downarrow}\, e^{ik_{zp2}H} + B^{II}_{P_\downarrow S_\downarrow}\, e^{ik_{zs2}H}] \\ &+ \rho_f C_T^I \omega S(\omega) B_{21}(A^I_{P_\downarrow}, A^I_{P_\downarrow P_\uparrow}, A^I_{P_\downarrow S_\uparrow})\, e^{ik_{c2}H} \\ &+ \rho_f C_T^{II} \omega S(\omega) B_{22}(A^{II}_{P_\downarrow P_\downarrow}, A^{II}_{P_\downarrow S_\downarrow})\, e^{ik_{c2}H} \end{aligned} \tag{4}$$

where $k_{c1} = \omega/C_T^I$ and $k_{c2} = \omega/C_T^{II}$. It is worthwhile to note that when the layer does not exist, all the coefficients are zero except $B^I_{P_\downarrow}$ and $B^{II}_{P_\downarrow P_\downarrow}$.

Application of the Negative Dislocation Theory

When the borehole goes through two media, there are different coupling effects between the incoming wave and the borehole in the upper and lower media. To deal with the discontinuity, a negative dislocation source can be added at the boundary to compensate for the discontinuity. Then the problem can be divided into three parts, as shown in Figure 1: two half-spaces, two boreholes one in each half-space, and sources along the interface and the borehole generating the tube waves. For the generation of the tube wave inside the borehole, the sources accounting for the discontinuity in the formation contribute significantly less than that inside the fluid. This is because the amplitude of the eigenfunction of tube wave displacement inside the borehole is significantly larger than that outside (Cheng and Toksöz, 1984).

The displacement and stress discontinuity at $z = 0$ (layer boundary) inside the borehole can be written as

$$[u_r^f(r)] = -\alpha_f \sum_{n=-\infty}^{n=\infty} i^n [U^f_{rn}(r)] \cos n\theta$$

$$[u_\theta^f(r)] = \alpha_f \sum_{n=-\infty}^{n=\infty} i^n [U^f_{\theta_n}(r)] \sin n\theta$$

$$[u_z^f(r)] = -\alpha_f \sum_{n=-\infty}^{n=\infty} i^n [U^f_{zn}(r)] \cos n\theta$$

$$[\sigma_{zz}^f(r)] = -\rho_f \alpha_f \sum_{n=-\infty}^{n=\infty} i^n [R_{fn}(r)] \cos n\theta$$

where $[U^f_{rn}(r)]$,$[U^f_{\theta_n}(r)]$, $[U^f_{zn}(r)]$ and $[R_{fn}(r)]$ are related to the reflection and transmission coefficients and formation as well as incident wave properties.

By employing the elastic representation theory (Aki and Richards, 1980) in the frequency domain, we can derive the contribution of the secondary sources at position $\vec{x}$ as (Figure 2)

$$u_n(\vec{x}) = -\int\int_S \{G_{3n}(\vec{\xi},\vec{x})[\sigma^f_{zz}(\vec{\xi})] - \rho_f\alpha_f^2([u^f_r(\vec{\xi})] + [u^f_\theta(\vec{\xi})] + [u^f_z(\vec{\xi})])\frac{\partial G_{kn}}{\partial \xi_k}(\vec{\xi},\vec{x})\}dS(\vec{\xi}). \tag{5}$$

The free-space Green's tensor in the fluid can be written as

$$\underline{\underline{G}}(\vec{x},\vec{x}') = \frac{1}{4\pi\rho_f\omega^2}\underline{\nabla} g_P(\vec{x},\vec{x}')\underline{\nabla}'$$

where

$$g_P(\vec{x},\vec{x}') = \frac{e^{i\omega/\alpha_f R}}{R} = \frac{1}{2\pi}\int_{-\infty}^{\infty}[i\pi H_0^{(1)}(k_f\bar{r})]\, e^{ik_z z}dk_z.$$

Integration in (5) can be evaluated exactly and the displacement due to the secondary source is equivalent to that generated by a source with potential

$$\phi_f(r,\theta,z) = \frac{\alpha_f}{4i}\int_{-\infty}^{\infty} e^{ik_z z}dk_z \sum_{m=0}^{\infty}\varepsilon_m i^m[\Phi^c_m(r)\cos m\theta + \Phi^s_m(r)\sin m\theta]. \tag{6}$$

Again, Φ^c_m and Φ^s_m are related to the transmission and reflection coefficients and the formation as well as incident wave properties. Details are given in the appendix B.

Given the source potential, the classical solution (Cheng and Toksöz, 1981) can be applied to compute the borehole excitation.

Sensitivity of the Tube Wave to the Formation Parameter

The reflection and transmission coefficient for the plane wave incident upon the layer boundary can be expanded in terms of formation properties contrasts $\frac{\Delta\rho}{\rho}$, $\frac{\Delta\beta}{\beta}$ and $\frac{\Delta\alpha}{\alpha}$ to the first order (Richards and Frasier, 1976; Chapman, 1976). For the case of P-wave incidence, the ratio of the amplitude of pressure of the reflected tube wave to that of the incident P wave can be written as

$$\frac{P^R_{tube}}{P_{inc}} = R_\rho\frac{\Delta\rho}{\rho} + R_\beta\frac{\Delta\beta}{\beta} + R_\alpha\frac{\Delta\alpha}{\alpha} \tag{7}$$

where R_ρ, R_β and R_α are the sensitivity functions of the reflected tube wave to the density, shear, and compressional velocity contrasts, respectively. Details are given in the appendix C.

As a function of the incident angle, we plot these sensitivity functions for the case $\alpha = 5970\, m/s$, $\beta = 2880\, m/s$ and $\rho = 2656\, Kg/m^3$ (Solenhofen Limestone) as shown in Figure 3. We see that the reflected tube wave is more sensitive to the shear velocity contrast across the layer boundary than those of density and compressional velocities. In addition, R_α shows a negative sign to R_β and R_ρ for this particular choice of parameters.

NUMERICAL EXAMPLES

The first example shows that the zero frequency approximation and the negative dislocation theory agree when the frequency is low. In this calculation, $\alpha_1 = 5970\, m/s$, $\beta_1 = 2880 m/s$, $\rho_1 = 2656 Kg/m^3$ and $\alpha_2 = 4206 m/s$, $\beta_2 = 2664 m/s$, $\rho_2 = 2140 Kg/m^3$, which mimics the (Solenhofen) limestone formation embedded above the (Berea) sandstone. The borehole fluid is water and the radius is 10 cm. The frequency of the incident P wave is 100 Hz and the incident angle is 25°. The offset of the receiver is 100 m from the layer boundary and the time window is 250 ms. Figure 4 shows that excellent agreement can be found, especially when they are plotted on top of each other (Figure 5). The small artifact in the negative dislocation approach comes from the imaginary source of the Discrete Wavenumber Method. It is interesting to note that the reflected and transmitted tube waves generated at a layer boundary show opposite polarities, which is different from those generated from a fracture.

If the source frequency is increased to 1000 Hz and other parameters are kept the same, a discrepancy can be observed from these two approaches, as shown in Figure 6. In this case the zero frequency approximation is inaccurate.

In the third example (Figure 7), we assign the same density and compressional velocity to medium #1 and medium #2 and vary the shear velocity of medium #2. In this calculation, all other parameters remain the same as in the first example, except $\alpha_2 = 5970\, m/s$, $\beta_2 = 4320\, m/s$, and $\rho_2 = 2656\, Kg/m^3$ (i.e., 50% perturbation in shear velocity). The large amplitude-reflected tube wave is generated from the layer boundary. From the sensitivity analysis we might expect an even larger amplitude tube wave (0.8 times the incident wave), but we should remember that the sensitivity analysis is based on the first-order approximation.

The fourth example (Figure 8) is the same as the third example, except $\alpha_2 = 8955 m/s$, $\beta_2 = 2880 m/s$, and $\rho_2 = 2656 Kg/m^3$ (i.e., 50% perturbation in compressional velocity). In this case, the reflected tube wave has an opposite polarity compared to the third example. Also, the reflected tube wave is nearly half the amplitude of that in Figure 7.

In the fifth example (Figure 9), $\alpha_2 = 5970 m/s$, $\beta_2 = 2880 m/s$, and $\rho_2 = 3984 Kg/m^3$

(i.e., 50% perturbation in density). The reflected tube wave is slightly less than that in the fourth example and has the same polarity as the third example.

In the sixth example (Figure 10), $\alpha_2 = 8955\ m/s$, $\beta_2 = 3600\ m/s$, and $\rho_2 = 2656\ Kg/m^3$ (i.e., 50% perturbation in compressional velocity and 25% in shear velocity). In this case, we should expect little reflected tube wave because of the cancellation of the tube wave contributed by shear velocity perturbation with that by compressional velocity perturbation. This is indeed true.

COMPARISON WITH FINITE DIFFERENCE

Using the Finite difference method, it is feasible to model wave propagation in cylindrical coordinate with azimuthal symmetry. A finite difference scheme based on a velocity-stress formulation is developed by Cheng et al. (this issue) to study energy radiation into the formation from a fluid-filled borehole. It can also be used to study borehole interaction with the formation for a ring source inside the solid. In Appendix D, we have proved that up to a constant factor, the pressure at the center of fluid excited by a ring source is equivalent to that by an incident plane P wave, as long as the radius of the ring source is large compared to the radius of the borehole and the aperture of the measurement is small. This justifies the comparison of finite difference calculations with the results from the negative dislocation approach when the equivalence conditions hold.

The model used for the comparison is a 20 cm diameter borehole drilled through a lucite ($\alpha_1 = 2700\ m/s$, $\beta_1 = 1400\ m/s$, and $\rho_1 = 2000\ Kg/m^3$) and aluminium ($\alpha_2 = 6300 m/s$, $\beta_2 = 3400 m/s$, and $\rho_2 = 2700 Kg/m^3$) formations. The layer boundary is at $z = 2.56\ m$ and 32 hydrophones are evenly distributed at the center of borehole from $z_1 = 1.6\ m$ to $z_2 = 4.7\ m$. The source is chosen to be a Kelly wavelet with a center frequency of 2 kHz. In the finite difference simulation, the ring source is located at ($r_0 = 2.0\ m$, $z_0 = 0$) which corresponds approximately to $\delta = 37^o$ incidence at the layer boundary. The implememtation is acomplished on an nCUBE parallel computer with 64 nodes and takes approximately 30 minutes. In the calculation by negative dislocation approach, an plane P wave incidence at $\delta = 37^o$ is assumed. The computation time on an Vax 8800 is nearly 20 minutes. Calculations by the finite difference technique is shown in Figure 11a, from which we can see the incident P wave and reflected S wave in the lucite formation and transmitted S wave and strong tube wave (phase velocity around 1426.0 m/s) in the aluminium formation. We can also see the incident S wave and reflected S wave and the tube wave generated by the S wave incidence at a later time, as well as some boundary reflections behind 4 ms. These waves should not exist if perfect boundary conditions and pure volume source is achieved in the finite difference calculation. The calculation by the negative dislocation theory is shown in Figure 11b. Compared to the P wave incidence portion of finite difference result, we see excellent

agreement between these two approaches.

CONCLUSIONS

Two approaches—zero frequency approximation and negative dislocation theory—are examined for the calculation of tube wave generation at a layer boundary when a plane compressional wave incidents upon the borehole. Excellent agreement of these two approaches is found when the source frequency is below hundreds of Hertz and a significant tube wave can be generated when the contrast of elastic properties across the layer boundary is large. For frequencies up to one kilohertz, the zero frequency approximation fails to be valid, whereas the negative dislocation approach is still a good approximation. At a low frequency, the excited tube wave is independent of the borehole radius and shows stronger sensitivity to the formation shear velocity contrast compared to that of the compressional velocity and density, and the sensitivity toward the compressional velocity is opposite those of shear velocity and density. Unlike those excited by a fracture, for a plane P wave incidence the reflected and transmitted tube waves generated at a layer boundary show opposite polarities. Examples of calculations support these conclusions.

These methods can also be applied to the case of shear wave incidence and can be generalized to the case of a stack of layers and an arbitrary source by employing the well-known discrete wavenumber approach (Bouchon, 1977).

ACKNOWLEDGEMENTS

The work was supported by the Borehole Acoustics and Logging Consortium at M.I.T. Chengbin Peng is also supported by an nCUBE graduate student fellowship. Part of the computing was performed at the ERL/nCUBE Geophysical Center for Parallel Processing. We are grateful to Ningya Cheng for the use of his finite difference code.

REFERENCES

Aki, K., and P.G. Richards, 1980, *Quantitative seismology: theory and methods, volume 1,* W.H. Freeman and Company, New York.

Biot, M., 1952, Propagation of elastic waves in a cylindrical borehole containing a fluid, *J. Appl. Phys., 23,* 997–1009 . Bouchon, M., and K. Aki, 1977, Discrete wavenumber representation of seismic source wave field, *Bull. Seism. Soc. Am., 67,* 259–277.

Chapman, C.H., 1976, Exact and approximate generalized ray theory in vertically inhomogeneous media, *Geophy. J. Roy. Astr. Soc., 46,* 201–233.

Cheng, C.H., and M.N. Toksöz, 1981, Elastic wave propagation in a fluid-filled borehole and synthetic acoustic logs, *Geophysics, 46,* 1042–1053.

Cheng, C.H., and M.N. Toksöz, 1984, Generation, propagation and analysis of tube waves in a borehole, *in Vertical Seismic Profiling, 14B,* 276–287, Geophysical Press.

Morse, P.M., and H. Feshbach, 1953, *Methods of theoretical physics, Part I,* McGraw-Hill, New York.

Peng, C., Cheng, C.H., and M.N. Toksöz, Borehole effects on downhole seismic measurements, *this volume.*

Richards, P.G., and C.W. Frasier, 1976, Scattering of elastic waves from depth-dependent inhomogeneities, *Geophysics, 41,* 441–458.

Schoenberg, M., 1986, Fluid and solid motion in the neighborhood of a fluid-filled borehole due to the passage of a low-frequency elastic plane wave, *Geophysics, 51,* 1191–1205.

Timoshenko, S., and J.N. Goodier, 1951, *Theory of Elasticity,* McGraw-Hill, New York.

White, J.E., 1953, Signals in a borehole due to plane waves in the solid, *J. Acoust. Soc. Am., 25,* 906–915.

White, J.E., 1983, *Underground Sound,* Elsevier.

Appendix A. ZERO FREQUENCY APPROXIMATION

When a plane P wave incidents upon the layer boundary from medium #1, in the case that no borehole exists, there will be reflected plane P and S waves in medium #1 and transmitted plane P and S waves in medium #2. The displacement reflection and transmittion coefficients can be found in many places in the literature such as Aki and Richards (1980). We will follow the notations used by Aki and Richards in this paper.

Suppose the polarization and propagation directions are confined in the (x, z) plane. The normal stresses σ_{xx}, σ_{yy} and σ_{zz} due to these plane waves can be written as

$$\begin{aligned}
\sigma^I_{xx} &= \lambda_1 iS(\omega)\,[k_{\alpha 1}\, e^{i(k_{p1}x+k_{zp1}z)} + P_\downarrow P_\uparrow\, k_{\alpha 1}\, e^{i(k_{p1}x-k_{zp1}z)}] + 2\mu_1 iS(\omega)\,[\frac{k^2_{p1}}{k_{\alpha 1}}\, e^{i(k_{p1}x+k_{zp1}z)} \\
&\quad + P_\downarrow P_\uparrow\, \frac{k^2_{p1}}{k_{\alpha 1}}\, e^{i(k_{p1}x-k_{zp1}z)} + P_\downarrow S_\uparrow\, \frac{k_{s1}k_{zs1}}{k_{\beta 1}}\, e^{i(k_{s1}x-k_{zs1}z)}] \\
\sigma^I_{yy} &= \lambda_1 iS(\omega)\,[k_{\alpha 1}\, e^{i(k_{p1}x+k_{zp1}z)} + P_\downarrow P_\uparrow\, k_{\alpha 1}\, e^{i(k_{p1}x-k_{zp1}z)}] \\
\sigma^I_{zz} &= \lambda_1 iS(\omega)\,[k_{\alpha 1}\, e^{i(k_{p1}x+k_{zp1}z)} + P_\downarrow P_\uparrow\, k_{\alpha 1}\, e^{i(k_{p1}x-k_{zp1}z)}] + 2\mu_1 iS(\omega)\,[\frac{k^2_{zp1}}{k_{\alpha 1}}\, e^{i(k_{p1}x+k_{zp1}z)} \\
&\quad + P_\downarrow P_\uparrow\, \frac{k^2_{zp1}}{k_{\alpha 1}}\, e^{i(k_{p1}x-k_{zp1}z)} - P_\downarrow S_\uparrow\, \frac{k_{s1}k_{zs1}}{k_{\beta 1}}\, e^{i(k_{s1}x-k_{zs1}z)}]
\end{aligned}$$

in medium #1, and

$$\begin{aligned}
\sigma^{II}_{xx} &= \lambda_2 iS(\omega)\, P_\downarrow P_\downarrow\, k_{\alpha 2}\, e^{i(k_{p2}x+k_{zp2}z)} + 2\mu_2 iS(\omega)\,[P_\downarrow P_\downarrow\, \frac{k^2_{p2}}{k_{\alpha 2}}\, e^{i(k_{p2}x+k_{zp2}z)} \\
&\quad + P_\downarrow S_\downarrow\, \frac{k_{s2}k_{zs2}}{k_{\beta 2}}\, e^{i(k_{s2}x+k_{zs2}z)}] \\
\sigma^{II}_{yy} &= \lambda_2 iS(\omega)\, P_\downarrow P_\downarrow\, k_{\alpha 2}\, e^{i(k_{p2}x+k_{zp2}z)} \\
\sigma^{II}_{zz} &= \lambda_2 iS(\omega)\, P_\downarrow P_\downarrow\, k_{\alpha 2}\, e^{i(k_{p2}x+k_{zp2}z)} + 2\mu_2 iS(\omega)\,[P_\downarrow P_\downarrow\, \frac{k^2_{zp2}}{k_{\alpha 2}}\, e^{i(k_{p2}x+k_{zp2}z)} \\
&\quad - P_\downarrow S_\downarrow\, \frac{k_{s2}k_{zs2}}{k_{\beta 2}}\, e^{i(k_{s2}x+k_{zs2}z)}]
\end{aligned}$$

in medium #2. Where

$$
\begin{aligned}
&k_{p1} = \frac{\omega}{\alpha_1}\sin i_1 = \omega p, && k_{s1} = \frac{\omega}{\beta_1}\sin j_1 = \omega p,\\
&k_{zp1} = \frac{\omega}{\alpha_1}\cos i_1 = \sqrt{k_{\alpha 1}^2 - k_{p1}^2}, && k_{zs1} = \frac{\omega}{\beta_1}\cos j_1 = \sqrt{k_{\beta 1}^2 - k_{s1}^2},\\
&k_{\alpha 1} = \frac{\omega}{\alpha_1}, && k_{\beta 1} = \frac{\omega}{\beta_1};\\
&k_{p2} = \frac{\omega}{\alpha_2}\sin i_2 = \omega p, && k_{s2} = \frac{\omega}{\beta_2}\sin j_2 = \omega p,\\
&k_{zp2} = \frac{\omega}{\alpha_2}\cos i_2 = \sqrt{k_{\alpha 2}^2 - k_{p2}^2}, && k_{zs2} = \frac{\omega}{\beta_2}\cos j_2 = \sqrt{k_{\beta 2}^2 - k_{s2}^2},\\
&k_{\alpha 2} = \frac{\omega}{\alpha_2}, && k_{\beta 2} = \frac{\omega}{\beta_2}.
\end{aligned}
$$

and where p is the ray parameter, i and j are defined in terms of ray direction with the vertical axis for the plane P and S waves respectively. λ_1 and μ_1 are Lamé parameters in medium #1 and λ_2 and μ_2 are Lamé parameters in medium #2

Under the zero frequency approximation, the size of the borehole is much smaller than the wavelength such that the stresses generated by the incident wave are nearly homogeneous at the vicinity around the borehole (much larger than the borehole radius, but much smaller than the wavelength) if the borehole does not exist. Introduction of a borehole will locally disturb the homogeneous stress field at the expense of borehole deformation. The volume change of the borehole sets up a pressure inside the fluid in the same way as a piston source does (White, 1983). The change of borehole radius due to the stress field of incident elastic waves can be calculated by first computing the axial strain in the formation

$$\frac{\partial u_r}{\partial r} = \frac{1}{E}[\sigma_{rr} - \nu\sigma_{\theta\theta} - \nu\sigma_{zz}] \tag{A-1}$$

where

$$
\begin{aligned}
\sigma_{rr} &= \frac{\sigma_{xx}+\sigma_{yy}}{2}(1-\frac{a^2}{r^2}) + \frac{\sigma_{xx}-\sigma_{yy}}{2}(1+\frac{3a^4}{r^4}-\frac{4a^2}{r^2})\cos 2\theta\\
\sigma_{\theta\theta} &= \frac{\sigma_{xx}+\sigma_{yy}}{2}(1+\frac{a^2}{r^2}) - \frac{\sigma_{xx}-\sigma_{yy}}{2}(1+\frac{3a^4}{r^4})\cos 2\theta
\end{aligned}
$$

are the stress fields near the borehole (Timoshenko and Goodier, 1951) and E denotes the Young's modulus. Integration of (A-1) yields

$$u_r = \frac{a}{E}[(\sigma_{xx}+\sigma_{yy}) + 2(\sigma_{xx}-\sigma_{yy})\cos 2\theta - \nu\sigma_{zz}] \tag{A-2}$$

at $r = a$.

Excitation of pressure inside the fluid is only dependent on the axial symmetric component $\bar{u}_r$ of (A-2), i.e.,

$$\bar{u}_r = \frac{1}{2\pi}\int_0^{2\pi} u_r d\theta.$$

The change of borehole average radius will lead to a vertical motion of fluid. Consider a differential section dz along the borehole, the differential vertical velocity $d\bar{v}$ of fluid motion can be related to the rate of change of borehole radius by the law of conservation of fluid mass, i.e.,

$$2\pi a^2 d\bar{v} = -2\pi a dz \frac{d\bar{u}_r}{dt}$$

from which we can get

$$\frac{d\bar{v}}{dz} = i\omega \frac{\bar{u}_r}{a}. \tag{A-3}$$

In the fluid, pressure and particle velocity are related by

$$dp = \rho_f C_T d\bar{v}$$

where ρ_f is the fluid density and C_T is the zero frequency tube wave velocity given by (Boit, 1952; White, 1983)

$$C_T = \frac{\alpha_f}{\sqrt{1 + \frac{\rho_f \alpha_f^2}{\rho \beta^2}}}.$$

Following these steps, we can obtain

$$dP_I = \rho_f C_T^I \omega S(\omega) \left[A^I_{P_\downarrow} e^{ik_{zp1}z} + A^I_{P_\downarrow P_\uparrow} e^{-ik_{zp1}z} + A^I_{P_\downarrow S_\uparrow} e^{-ik_{zs1}z}\right] dz, \tag{A-4}$$

in medium #1, and

$$dP_{II} = \rho_f C_T^{II} \omega S(\omega) \left[A^{II}_{P_\downarrow P_\downarrow} e^{ik_{zp2}z} + A^{II}_{P_\downarrow S_\downarrow} e^{ik_{zs2}z}\right] dz \tag{A-5}$$

in medium #2, where

$$\begin{aligned}
A^I_P &= \{[\, k_{\alpha 1}(2-\nu_1)\frac{\lambda_1}{E_1} + \frac{k_{p1}^2}{k_{\alpha 1}}(2-2\nu_1)\frac{\mu_1}{E_1}\,]J_0(k_{p1}a) - \frac{k_{p1}^2}{k_{\alpha 1}}\frac{4\mu_1}{E_1}J_2(k_{p1}a)\} \\
A^I_{P_\downarrow P_\uparrow} &= \{[\, k_{\alpha 1}(2-\nu_1)\frac{\lambda_1}{E_1} + \frac{k_{p1}^2}{k_{\alpha 1}}(2-2\nu_1)\frac{\mu_1}{E_1}\,]J_0(k_{p1}a) - \frac{k_{p1}^2}{k_{\alpha 1}}\frac{4\mu_1}{E_1}J_2(k_{p1}a)\}\, P_\downarrow P_\uparrow \\
A^I_{P_\downarrow S_\uparrow} &= \{\frac{k_{s1}k_{zs1}}{k_{\beta 1}}\frac{2\mu_1}{E_1}[J_0(k_{s1}a) - 2J_2(k_{s1}a) + \nu_1 J_0(k_{s1}a)]\}\, P_\downarrow S_\uparrow
\end{aligned}$$

$$\begin{aligned}
A^{II}_{P_\downarrow P_\downarrow} &= \{[\, k_{\alpha 2}(2-\nu_2)\frac{\lambda_2}{E_2} + \frac{k_{p2}^2}{k_{\alpha 2}}(2-2\nu_2)\frac{\mu_2}{E_2}\,]J_0(k_{p2}a) - \frac{k_{p2}^2}{k_{\alpha 2}}\frac{4\mu_2}{E_2}J_2(k_{p2}a)\}\, P_\downarrow P_\downarrow \\
A^{II}_{P_\downarrow S_\downarrow} &= \{\frac{k_{s2}k_{zs2}}{k_{\beta 2}}\frac{2\mu_2}{E_2}[J_0(k_{s2}a) - 2J_2(k_{s2}a) + \nu_2 J_0(k_{s2}a)]\}\, P_\downarrow S_\downarrow
\end{aligned}$$

For a point at $z = H(H < 0)$ in medium #1, the total pressure and axial velocity are built up as

$$\begin{aligned} P(H<0,\omega) &= \int_{-\infty}^{H} dP_I(z,\omega)\, e^{ik_{c1}(H-z)} + \int_{H}^{0} dP_I(z,\omega)\, e^{ik_{c1}(z-H)} \\ &\quad + \int_{0}^{\infty} dP_{II}(z,\omega)\, e^{i(k_{c2}z - k_{c1}H)} \\ V(H<0,\omega) &= \int_{-\infty}^{H} d\bar{v}_I(z,\omega)\, e^{ik_{c1}(H-z)} - \int_{H}^{0} d\bar{v}_I(z,\omega)\, e^{ik_{c1}(z-H)} \\ &\quad - \int_{0}^{\infty} d\bar{v}_{II}(z,\omega)\, e^{i(k_{c2}z - k_{c1}H)} \end{aligned}$$

where $k_{c1} = \omega/C_T^I$ and $k_{c2} = \omega/C_T^{II}$.

For the same reason, for a point at $z = H(H > 0)$ in medium #2, we have

$$\begin{aligned} P(H>0,\omega) &= \int_{-\infty}^{0} dP_I(z,\omega)\, e^{i(-k_{c1}z + k_{c2}H)} + \int_{0}^{H} dP_{II}(z,\omega)\, e^{ik_{c2}(H-z)} \\ &\quad + \int_{H}^{\infty} dP_{II}(z,\omega)\, e^{ik_{c2}(z-H)} \\ V(H>0,\omega) &= \int_{-\infty}^{0} d\bar{v}_I(z,\omega)\, e^{i(-k_{c1}z + k_{c2}H)} + \int_{0}^{H} d\bar{v}_{II}(z,\omega)\, e^{ik_{c2}(H-z)} \\ &\quad - \int_{H}^{\infty} d\bar{v}_{II}(z,\omega)\, e^{ik_{c2}(z-H)}. \end{aligned}$$

The integrations can be exactly carried out and terms associated with infinite time delay are excluded (White, 1953). We finally come up with (3) and (4) for pressures and the following for axial velocity:

$$\begin{aligned} V(H<0,\omega) &= \omega S(\omega)[D^I_{P_\downarrow}\, e^{ik_{zp1}H} + D^I_{P_\downarrow P_\uparrow}\, e^{-ik_{zp1}H} + D^I_{P_\downarrow S_\uparrow}\, e^{-ik_{zs1}H}] \\ &+ \omega S(\omega) D_{11}(A^I_{P_\downarrow}, A^I_{P_\downarrow P_\uparrow}, A^I_{P_\downarrow S_\uparrow})\, e^{-ik_{c1}H} \\ &+ \omega S(\omega) D_{12}(A^{II}_{P_\downarrow P_\downarrow}, A^{II}_{P_\downarrow S_\downarrow})\, e^{-ik_{c1}H} \end{aligned} \tag{A-6}$$

and

$$\begin{aligned} V(H>0,\omega) &= \omega S(\omega)[D^{II}_{P_\downarrow P_\downarrow}\, e^{ik_{zp2}H} + D^{II}_{P_\downarrow S_\downarrow}\, e^{ik_{zs2}H}] \\ &+ \omega S(\omega) D_{21}(A^I_{P_\downarrow}, A^I_{P_\downarrow P_\uparrow}, A^I_{P_\downarrow S_\uparrow})\, e^{ik_{c2}H} \\ &+ \omega S(\omega) D_{22}(A^{II}_{P_\downarrow P_\downarrow}, A^{II}_{P_\downarrow S_\downarrow})\, e^{ik_{c2}H} \end{aligned} \tag{A-7}$$

where

$$B^I_{P_\downarrow} = 2i \frac{k_{c1}}{k_{c1}^2 - k_{zp1}^2} A^I_{P_\downarrow}$$

$$B^I_{P_\downarrow P_\uparrow} = 2i\frac{k_{c1}}{k_{c1}^2 - k_{zp1}^2} A^I_{P_\downarrow P_\uparrow}$$

$$B^I_{P_\downarrow S_\uparrow} = 2i\frac{k_{c1}}{k_{c1}^2 - k_{zs1}^2} A^I_{P_\downarrow S_\uparrow}$$

$$B_{11} = -i\left(\frac{A^I_{P_\downarrow}}{k_{c1} + k_{zp1}} + \frac{A^I_{P_\downarrow P_\uparrow}}{k_{c1} - k_{zp1}} + \frac{A^I_{P_\downarrow S_\uparrow}}{k_{c1} - k_{zs1}}\right)$$

$$B_{12} = i\left(\frac{A^{II}_{P_\downarrow P_\downarrow}}{k_{c2} + k_{zp2}} + \frac{A^{II}_{P_\downarrow S_\downarrow}}{k_{c2} + k_{zs2}}\right)$$

$$B^{II}_{P_\downarrow P_\downarrow} = 2i\frac{k_{c2}}{k_{c2}^2 - k_{zp2}^2} A^{II}_{P_\downarrow P_\downarrow}$$

$$B^{II}_{P_\downarrow S_\downarrow} = 2i\frac{k_{c2}}{k_{c2}^2 - k_{zs2}^2} A^{II}_{P_\downarrow S_\downarrow}$$

$$B_{21} = i\left(\frac{A^I_{P_\downarrow}}{k_{c1} - k_{zp1}} + \frac{A^I_{P_\downarrow P_\uparrow}}{k_{c1} + k_{zp1}} + \frac{A^I_{P_\downarrow S_\uparrow}}{k_{c1} + k_{zs1}}\right)$$

$$B_{22} = -i\left(\frac{A^{II}_{P_\downarrow P_\downarrow}}{k_{c2} - k_{zp2}} + \frac{A^{II}_{P_\downarrow S_\downarrow}}{k_{c2} - k_{zs2}}\right)$$

$$D^I_{P_\downarrow} = 2i\frac{k_{zp1}}{k_{c1}^2 - k_{zp1}^2} A^I_{P_\downarrow}$$

$$D^I_{P_\downarrow P_\uparrow} = -2i\frac{k_{zp1}}{k_{c1}^2 - k_{zp1}^2} A^I_{P_\downarrow P_\uparrow}$$

$$D^I_{P_\downarrow S_\uparrow} = -2i\frac{k_{zs1}}{k_{c1}^2 - k_{zs1}^2} A^I_{P_\downarrow S_\uparrow}$$

$$D_{11} = i\left(\frac{A^I_{P_\downarrow}}{k_{c1} + k_{zp1}} + \frac{A^I_{P_\downarrow P_\uparrow}}{k_{c1} - k_{zp1}} + \frac{A^I_{P_\downarrow S_\uparrow}}{k_{c1} - k_{zs1}}\right)$$

$$D_{12} = -i\left(\frac{A^{II}_{P_\downarrow P_\downarrow}}{k_{c2} + k_{zp2}} + \frac{A^{II}_{P_\downarrow S_\downarrow}}{k_{c2} + k_{zs2}}\right)$$

$$D^{II}_{P_\downarrow P_\downarrow} = 2i\frac{k_{zp2}}{k_{c2}^2 - k_{zp2}^2} A^{II}_{P_\downarrow P_\downarrow}$$

$$D^{II}_{P_\downarrow S_\downarrow} = 2i\frac{k_{zs2}}{k_{c2}^2 - k_{zs2}^2} A^{II}_{P_\downarrow S_\downarrow}$$

$$D_{21} = i\left(\frac{A^I_{P_\downarrow}}{k_{c1}-k_{zp1}} + \frac{A^I_{P_\downarrow P_\uparrow}}{k_{c1}+k_{zp1}} + \frac{A^I_{P_\downarrow S_\uparrow}}{k_{c1}+k_{zs1}}\right)$$

$$D_{22} = -i\left(\frac{A^{II}_{P_\downarrow P_\downarrow}}{k_{c2}-k_{zp2}} + \frac{A^{II}_{P_\downarrow S_\downarrow}}{k_{c2}-k_{zs2}}\right)$$

Appendix B. NEGATIVE DISLOCATION THEORY

As frequency goes higher, the zero frequency approximation fails to be valid because it ignores the borehole scattered wave in the formation and does not acknowledge the radial variation of fluid motion inside the borehole. Schoenberg's theory (Schoenberg, 1986), on the other hand, can be applied to exactly solve the coupling of the incident plane wave into the borehole. In so doing, when the formation is layered, the displacements and stresses across the plane of the layer boundary will be discontinuous because of the different coupling in the upper and lower formations. A negative dislocation source can be added at the boundary to compensate for the discontinuity. The total field is the summation of those due to incident waves and that generated by the dislocation source.

Following the same notation as Peng et al., (this volume), we can express the displacements and stress inside the fluid, due to the incident P wave in medium #1, as

$$u^f_r = -\alpha_f \left[U^{P_\downarrow}_{r0}(r)A^{P_\downarrow}_0 + 2\sum_{n=1}^{\infty} i^n U^{P_\downarrow}_{rn}(r)A^{P_\downarrow}_n \cos n\theta\right]$$

$$u^f_\theta = -\alpha_f \left[U^{P_\downarrow}_{\theta 0}(r)A^{P_\downarrow}_0 + 2\sum_{n=1}^{\infty} i^n U^{P_\downarrow}_{\theta n}(r)A^{P_\downarrow}_n (-\sin n\theta)\right]$$

$$u^f_z = -\alpha_f \left[U^{P_\downarrow}_{z0}(r)A^{P_\downarrow}_0 + 2\sum_{n=1}^{\infty} i^n U^{P_\downarrow}_{zn}(r)A^{P_\downarrow}_n \cos n\theta\right]$$

$$\sigma^f_{zz} = -\rho_f\alpha_f \left[R^{P_\downarrow}_{f0}(r)A^{P_\downarrow}_0 + 2\sum_{n=1}^{\infty} i^n R^{P_\downarrow}_{fn}(r)A^{P_\downarrow}_n \cos n\theta\right]$$

where $U^{P_\downarrow}_{rn}(r) = k_{fp1}J'_n(k_{fp1}r)$, $U^{P_\downarrow}_{\theta n}(r) = n/r J_n(k_{fp1}r)$, $U^{P_\downarrow}_{zn}(r) = ik_{zp1}J_n(k_{fp1}r)$ and $R^{P_\downarrow}_{fn}(r) = -\omega^2 J_n(k_{fp1}r)$. Here $k_{fp1} = \sqrt{\omega^2/\alpha_f^2 - k_{zp1}^2}$ is the radial wavenumber in the

fluid. Time and depth dependence of the form $e^{i(k_z z-\omega t)}$ are assumed.

For the same reason, the displacements and stress inside the fluid, due to the reflected P wave in medium #1, can also be written as

$$\begin{aligned}
u_r^f &= -\alpha_f \left[U_{r0}^{P\downarrow P\uparrow}(r) A_0^{P\downarrow P\uparrow} + 2\sum_{n=1}^{\infty} i^n U_{rn}^{P\downarrow P\uparrow}(r) A_n^{P\downarrow P\uparrow} \cos n\theta\right] \\
u_\theta^f &= -\alpha_f \left[U_{\theta 0}^{P\downarrow P\uparrow}(r) A_0^{P\downarrow P\uparrow} + 2\sum_{n=1}^{\infty} i^n U_{\theta n}^{P\downarrow P\uparrow}(r) A_n^{P\downarrow P\uparrow} (-\sin n\theta)\right] \\
u_z^f &= -\alpha_f \left[U_{z0}^{P\downarrow P\uparrow}(r) A_0^{P\downarrow P\uparrow} + 2\sum_{n=1}^{\infty} i^n U_{zn}^{P\downarrow P\uparrow}(r) A_n^{P\downarrow P\uparrow} \cos n\theta\right] \\
\sigma_{zz}^f &= -\rho_f \alpha_f \left[R_{f0}^{P\downarrow P\uparrow}(r) A_0^{P\downarrow P\uparrow} + 2\sum_{n=1}^{\infty} i^n R_{fn}^{P\downarrow P\uparrow}(r) A_n^{P\downarrow P\uparrow} \cos n\theta\right]
\end{aligned}$$

where $U_{rn}^{P\downarrow P\uparrow}(r) = k_{fp1} J_n'(k_{fp1} r)$, $U_{\theta n}^{P\downarrow P\uparrow}(r) = n/r J_n(k_{fp1} r)$, $U_{zn}^{P\downarrow P\uparrow}(r) = -ik_{zp1} J_n(k_{fp1} r)$ and $R_{fn}^{P\downarrow P\uparrow}(r) = -\omega^2 J_n(k_{fp1} r)$.

The displacements and stress inside the fluid due to the reflected S wave in medium #1, cna be written as

$$\begin{aligned}
u_r^f &= -\alpha_f \left[U_{r0}^{P\downarrow S\uparrow}(r) A_0^{P\downarrow S\uparrow} + 2\sum_{n=1}^{\infty} i^n U_{rn}^{P\downarrow S\uparrow}(r) A_n^{P\downarrow S\uparrow} \cos n\theta\right] \\
u_\theta^f &= -\alpha_f \left[U_{\theta 0}^{P\downarrow S\uparrow}(r) A_0^{P\downarrow S\uparrow} + 2\sum_{n=1}^{\infty} i^n U_{\theta n}^{P\downarrow S\uparrow}(r) A_n^{P\downarrow S\uparrow} (-\sin n\theta)\right] \\
u_z^f &= -\alpha_f \left[U_{z0}^{P\downarrow S\uparrow}(r) A_0^{P\downarrow S\uparrow} + 2\sum_{n=1}^{\infty} i^n U_{zn}^{P\downarrow S\uparrow}(r) A_n^{P\downarrow S\uparrow} \cos n\theta\right] \\
\sigma_{zz}^f &= -\rho_f \alpha_f \left[R_{f0}^{P\downarrow S\uparrow}(r) A_0^{P\downarrow S\uparrow} + 2\sum_{n=1}^{\infty} i^n R_{fn}^{P\downarrow S\uparrow}(r) A_n^{P\downarrow S\uparrow} \cos n\theta\right]
\end{aligned}$$

where $U_{rn}^{P\downarrow S\uparrow}(r) = k_{fs1} J_n'(k_{fs1} r)$, $U_{\theta n}^{P\downarrow S\uparrow}(r) = n/r J_n(k_{fs1} r)$, $U_{zn}^{P\downarrow S\uparrow}(r) = -ik_{zs1} J_n(k_{fs1} r)$ and $R_{fn}^{P\downarrow S\uparrow}(r) = -\omega^2 J_n(k_{fs1} r)$.

For the transmitted P and S waves in medium #2, we have similar expressions

$$u_r^f = -\alpha_f \left[U_{r0}^{P\downarrow P\downarrow}(r) A_0^{P\downarrow P\downarrow} + 2\sum_{n=1}^{\infty} i^n U_{rn}^{P\downarrow P\downarrow}(r) A_n^{P\downarrow P\downarrow} \cos n\theta\right]$$

$$u_\theta^f = -\alpha_f \left[U_{\theta 0}^{P_\downarrow P_\downarrow}(r) A_0^{P_\downarrow P_\downarrow} + 2 \sum_{n=1}^{\infty} i^n U_{\theta n}^{P_\downarrow P_\downarrow}(r) A_n^{P_\downarrow P_\downarrow}(-\sin n\theta)\right]$$

$$u_z^f = -\alpha_f \left[U_{z0}^{P_\downarrow P_\downarrow}(r) A_0^{P_\downarrow P_\downarrow} + 2 \sum_{n=1}^{\infty} i^n U_{zn}^{P_\downarrow P_\downarrow}(r) A_n^{P_\downarrow P_\downarrow} \cos n\theta\right]$$

$$\sigma_{zz}^f = -\rho_f \alpha_f \left[R_{f0}^{P_\downarrow P_\downarrow}(r) A_0^{P_\downarrow P_\downarrow} + 2 \sum_{n=1}^{\infty} i^n R_{fn}^{P_\downarrow P_\downarrow}(r) A_n^{P_\downarrow P_\downarrow} \cos n\theta\right]$$

and

$$u_r^f = -\alpha_f \left[U_{r0}^{P_\downarrow S_\downarrow}(r) A_0^{P_\downarrow S_\downarrow} + 2 \sum_{n=1}^{\infty} i^n U_{rn}^{P_\downarrow S_\downarrow}(r) A_n^{P_\downarrow S_\downarrow} \cos n\theta\right]$$

$$u_\theta^f = -\alpha_f \left[U_{\theta 0}^{P_\downarrow S_\downarrow}(r) A_0^{P_\downarrow S_\downarrow} + 2 \sum_{n=1}^{\infty} i^n U_{\theta n}^{P_\downarrow S_\downarrow}(r) A_n^{P_\downarrow S_\downarrow}(-\sin n\theta)\right]$$

$$u_z^f = -\alpha_f \left[U_{z0}^{P_\downarrow S_\downarrow}(r) A_0^{P_\downarrow S_\downarrow} + 2 \sum_{n=1}^{\infty} i^n U_{zn}^{P_\downarrow S_\downarrow}(r) A_n^{P_\downarrow S_\downarrow} \cos n\theta\right]$$

$$\sigma_{zz}^f = -\rho_f \alpha_f \left[R_{f0}^{P_\downarrow S_\downarrow}(r) A_0^{P_\downarrow S_\downarrow} + 2 \sum_{n=1}^{\infty} i^n R_{fn}^{P_\downarrow S_\downarrow}(r) A_n^{P_\downarrow S_\downarrow} \cos n\theta\right]$$

where

$U_{rn}^{P_\downarrow P_\downarrow}(r) = k_{fp2} J_n'(k_{fp2} r)$, $U_{\theta n}^{P_\downarrow P_\downarrow}(r) = n/r J_n(k_{fp2} r)$, $U_{zn}^{P_\downarrow P_\downarrow}(r) = i k_{zp2} J_n(k_{fp2} r)$, $R_{fn}^{P_\downarrow P_\downarrow}(r) = -\omega^2 J_n(k_{fp2} r)$; and $U_{rn}^{P_\downarrow S_\downarrow}(r) = k_{fs2} J_n'(k_{fs2} r)$, $U_{\theta n}^{P_\downarrow S_\downarrow}(r) = n/r J_n(k_{fs2} r)$, $U_{zn}^{P_\downarrow S_\downarrow}(r) = i k_{zs2} J_n(k_{fs2} r)$, $R_{fn}^{P_\downarrow S_\downarrow}(r) = -\omega^2 J_n(k_{fs2} r)$.

The coefficients $A_n^{P_\downarrow}, A_n^{P_\downarrow P_\uparrow}, A_n^{P_\downarrow S_\uparrow}, A_n^{P_\downarrow P_\downarrow}, A_n^{P_\downarrow S_\downarrow}$ are obtained by matching the fluid-solid interface boundary conditions at the borehole wall (Peng et al., this volume).

The displacement and stress discontinuity at $z = 0$ (layer boundary) inside the borehole can be written as

$$[u_r^f(r)] = -\alpha_f \left\{ [U_{r0}^f(r)] + 2 \sum_{n=1}^{\infty} i^n [U_{rn}^f(r)] \cos n\theta \right\}$$

$$[u_\theta^f(r)] = -\alpha_f \left\{ [U_{\theta 0}^f(r)] + 2 \sum_{n=1}^{\infty} i^n [U_{\theta n}^f(r)] (-\sin n\theta) \right\}$$

$$[u_z^f(r)] = -\alpha_f \left\{ [U_{z0}^f(r)] + 2 \sum_{n=1}^{\infty} i^n [U_{zn}^f(r)] \cos n\theta \right\}$$

$$[\sigma_{zz}^f(r)] \;=\; -\rho_f\alpha_f\,\{\,[R_{fn}(r)] + 2\sum_{n=1}^{\infty} i^n\,[R_{fn}(r)]\,\cos n\theta\,\}. \tag{B-1}$$

where

$$[U_{rn}^f(r)] = U_{rn}^{P\downarrow P\downarrow}A_n^{P\downarrow P\downarrow} + U_{rn}^{P\downarrow S\downarrow}A_n^{P\downarrow S\downarrow} - U_{rn}^{P\downarrow}A_n^{P\downarrow} - U_{rn}^{P\downarrow P\uparrow}A_n^{P\downarrow P\uparrow} - U_{rn}^{P\downarrow S\uparrow}A_n^{P\downarrow S\uparrow}$$

$$[U_{\theta n}^f(r)] = U_{\theta n}^{P\downarrow P\downarrow}A_n^{P\downarrow P\downarrow} + U_{\theta n}^{P\downarrow S\downarrow}A_n^{P\downarrow S\downarrow} - U_{\theta n}^{P\downarrow}A_n^{P\downarrow} - U_{\theta n}^{P\downarrow P\uparrow}A_n^{P\downarrow P\uparrow} - U_{\theta n}^{P\downarrow S\uparrow}A_n^{P\downarrow S\uparrow}$$

$$[U_{zn}^f(r)] = U_{zn}^{P\downarrow P\downarrow}A_n^{P\downarrow P\downarrow} + U_{zn}^{P\downarrow S\downarrow}A_n^{P\downarrow S\downarrow} - U_{zn}^{P\downarrow}A_n^{P\downarrow} - U_{zn}^{P\downarrow P\uparrow}A_n^{P\downarrow P\uparrow} - U_{zn}^{P\downarrow S\uparrow}A_n^{P\downarrow S\uparrow}$$

$$[R_{fn}(r)] = R_{fn}^{P\downarrow P\downarrow}A_n^{P\downarrow P\downarrow} + R_{fn}^{P\downarrow S\downarrow}A_n^{P\downarrow S\downarrow} - R_{fn}^{P\downarrow}A_n^{P\downarrow} - R_{fn}^{P\downarrow P\uparrow}A_n^{P\downarrow P\uparrow} - R_{fn}^{P\downarrow S\uparrow}A_n^{P\downarrow S\uparrow}$$

A negative dislocation (displacement or stress discontinuity) of (B-1) must be applied at $z = 0$ to remove the discontinuity. The contribution of this secondary source can be evaluated by the elastic representation theory, which says (Aki and Richards, 1980)

$$u_n(\vec{x}) = \int\int_S [G_{in}(\vec{\xi};\vec{x})t_i(\vec{\xi}) - u_i(\vec{\xi})C_{ijkl}n_j\frac{\partial G_{kn}}{\partial \xi_k}(\vec{\xi};\vec{x})]ds(\vec{\xi}) \tag{B-2}$$

where t_i is the traction and u_i is the displacement on the surface.

For the isotropic case,

$$C_{ijkl} = \lambda\delta_{ij} + \mu(\delta_{ik}\delta_{jl} + \delta_{il}\delta_{jk}).$$

Substituting into (B-2), we obtain

$$u_n(\vec{x}) = \int\int_S [G_{3n}(\vec{\xi};\vec{x})t_3(\vec{\xi}) - \lambda_f\, n_i u_i(\vec{\xi})\frac{\partial G_{kn}}{\partial \xi_k}(\vec{\xi};\vec{x})]ds(\vec{\xi}) \tag{B-3}$$

in fluid ($\mu_f = 0$) with S corresponding to the area inside the fluid at $z = 0$.

The surface traction and displacements are related to the dislocation by

$$t_3(\vec{\xi}) = -[\sigma_{zz}^f(\vec{\xi})]$$

$$n_i u_i(\vec{\xi}) = -[u_r^f(\vec{\xi})] - [u_\theta^f(\vec{\xi})] - [u_z^f(\vec{\xi})]$$

from which we obtain

$$u_n(\vec{x}) = -\int\int_S \{G_{3n}(\vec{\xi},\vec{x})[\sigma_{zz}^f(\vec{\xi})] - \rho_f\alpha_f^2([u_r^f(\vec{\xi})] + [u_\theta^f(\vec{\xi})] + [u_z^f(\vec{\xi})])\frac{\partial G_{kn}}{\partial \xi_k}(\vec{\xi},\vec{x})\}dS(\vec{\xi}). \tag{B-4}$$

The free-space Green's tensor in the fluid can be written as

$$\underline{\underline{G}}(\vec{x},\vec{x}') = \frac{1}{4\pi\rho_f\omega^2}\underline{\nabla}g_P(\vec{x},\vec{x}')\underline{\nabla}'$$

where

$$g_P(\vec{x},\vec{x}') = \frac{e^{i\omega/\alpha_f R}}{R} = \frac{1}{2\pi}\int_{-\infty}^{\infty}[i\pi H_0^{(1)}(k_f\bar{r})]\, e^{ik_z z}dk_z$$

where $k_f^2+k_z^2 = \omega^2/\alpha_f^2$, $R^2 = (x-x')^2+(y-y')^2+(z-z')^2$ and $\bar{r}^2 = (x-x')^2+(y-y')^2$.

By making use of the following identities (Morse and Feshbach, 1953)

$$H_0^{(1)}(k_f\bar{r}) = \sum_{n=0}^{\infty}\varepsilon_n J_n(k_f r_<)H_n^{(1)}(k_f r_>)\cos n(\theta-\theta')$$

and

$$\frac{1}{\pi}\int_0^{2\pi}\cos n\theta'\cos m(\theta-\theta')d\theta' = \varepsilon_n^-\cos n\theta\delta_{mn},$$

where $r_< = min(r,r')$, $r_> = max(r,r')$ and $\varepsilon_n = \begin{cases} 1 & m=0 \\ 2 & m\neq 0 \end{cases}$ is the Neumann's factor and $\varepsilon_n^- = \begin{cases} 2 & m=0 \\ 1 & m\neq 0 \end{cases}$ is the inverse of the Neumann's factor, we obtain from (B-4)

$$u_n(\vec{x}) = \frac{\alpha_f}{4i}\frac{\partial}{\partial x_n}\int_{-\infty}^{\infty} e^{ik_z z}dk_z \sum_{m=0}^{\infty}\varepsilon_m i^m[\Phi_m^c(r)\cos m\theta + \Phi_m^s(r)\sin m\theta] \qquad \text{(B-5)}$$

where

$$\begin{aligned}\Phi_m^c(r) &= ik_z/\omega^2 f_m(r) - g_m^1(r) - g_m^3(r)\\ \Phi_m^s(r) &= g_m^2(r)\end{aligned}$$

and where

$$f_m(r) = H_m^{(1)}(k_f r)\int_0^r J_m(k_f r')[R_{fm}(r')]r'dr' + J_m(k_f r)\int_r^{r_b} H_m^{(1)}(k_f r')[R_{fm}(r')]r'dr'$$

$$g_m^1(r) = H_m^{(1)}(k_f r)\int_0^r J_m(k_f r')[U_{rm}^f(r')]r'dr' + J_m(k_f r)\int_r^{r_b} H_m^{(1)}(k_f r')[U_{rm}^f(r')]r'dr'$$

$$g_m^2(r) = H_m^{(1)}(k_f r)\int_0^r J_m(k_f r')[U_{\theta m}^f(r')]r'dr' + J_m(k_f r)\int_r^{r_b} H_m^{(1)}(k_f r')[U_{\theta m}^f(r')]r'dr'$$

$$g_m^3(r) = H_m^{(1)}(k_f r)\int_0^r J_m(k_f r')[U_{zm}^f(r')]r'dr' + J_m(k_f r)\int_r^{r_b} H_m^{(1)}(k_f r')[U_{zm}^f(r')]r'dr'$$

Taking the following transforms between cylindrical coordinates and rectangular coordinates,

$$\frac{\partial}{\partial x} = \cos\theta\frac{\partial}{\partial r} - \sin\theta\frac{1}{r}\frac{\partial}{\partial\theta}$$

$$\frac{\partial}{\partial y} = \sin\theta \frac{\partial}{\partial r} + \cos\theta \frac{1}{r}\frac{\partial}{\partial \theta}$$

we obtain

$$\begin{aligned} u_r &= \frac{\partial}{\partial r}\phi_f \\ u_\theta &= \frac{1}{r}\frac{\partial}{\partial \theta}\phi_f \\ u_z &= \frac{\partial}{\partial z}\phi_f \end{aligned}$$

where

$$\phi_f(r,\theta,z) = \frac{\alpha_f}{4i}\int_{-\infty}^{\infty} e^{ik_z z} dk_z \sum_{m=0}^{\infty} \varepsilon_m i^m [\Phi_m^c(r)\cos m\theta + \Phi_m^s(r)\sin m\theta]$$

is the equivalent displacement potential of the negative dislocation source.

Knowing the source potential, we can compute the borehole excitation by matching the fluid-solid interface boundary conditions. The classical solution can be found in Cheng and Toksöz (1981).

Appendix C. SENSITIVITY ANALYSIS

Consider a plane P wave incident on the layer boundary from medium #1. Denote α, β and ρ the elastic parameters in medium #1 and $\alpha+\Delta\alpha$, $\beta+\Delta\beta$ and $\rho+\Delta\rho$ the elastic parameters in medium #2. Let p be the ray parameter, i.e., $\sin i_1/\alpha = \sin j_1/\beta = \sin i_2/(\alpha+\Delta\alpha) = \sin j_2/(\beta+\Delta\beta) = p$, where i_1 and i_2 are the incidence angles of the P waves in medium #1 and #2 respectively, j_1 and j_2 are those of te S wave. Also let $i = (i_1+i_2)/2$ and $j = (j_1+j_2)/2$. Up to the first order of $\Delta\alpha/\alpha$, $\Delta\beta/\beta$ and $\Delta\rho/\rho$, Richards and Frasier (1976) had obtained

$$
\begin{aligned}
P_{\downarrow}P_{\uparrow} &= \frac{1}{2}(1-4\beta^2p^2)\frac{\Delta\rho}{\rho} + \frac{1}{2\cos^2 i}\frac{\Delta\alpha}{\alpha} - 4\beta^2p^2\frac{\Delta\beta}{\beta} \\
P_{\downarrow}S_{\uparrow} &= -\frac{p\alpha}{2\cos j}[(1-2\beta^2p^2+2\beta^2\frac{\cos i}{\alpha}\frac{\cos j}{\beta})\frac{\Delta\rho}{\rho} - (4\beta^2p^2-4\beta^2\frac{\cos i}{\alpha}\frac{\cos j}{\beta})\frac{\Delta\beta}{\beta}] \\
P_{\downarrow}P_{\downarrow} &= 1-\frac{1}{2}\frac{\Delta\rho}{\rho} + (\frac{1}{2\cos^2 i}-1)\frac{\Delta\alpha}{\alpha} \\
P_{\downarrow}S_{\downarrow} &= \frac{p\alpha}{2\cos j}[(1-2\beta^2p^2-2\beta^2\frac{\cos i}{\alpha}\frac{\cos j}{\beta})\frac{\Delta\rho}{\rho} - (4\beta^2p^2+4\beta^2\frac{\cos i}{\alpha}\frac{\cos j}{\beta})\frac{\Delta\beta}{\beta}].
\end{aligned}
$$

From equation (3), without the phase term $e^{i(\pi-k_{c1}H-k_{zp1}H)}$, the ratio of the pressure of the reflected tube wave to that of the incident wave can be written as

$$
\begin{aligned}
\frac{P^R_{tube}}{P_{inc}} &= \frac{k_{c1}-k_{zp1}}{2k_{c1}} + \frac{k_{c1}+k_{zp1}}{2k_{c1}}\frac{A^I_{P_{\downarrow}P_{\uparrow}}}{A^I_{P_{\downarrow}}} + \frac{k^2_{c1}-k^2_{zp1}}{2k_{c1}(k_{c1}-k_{zs1})}\frac{A^I_{P_{\downarrow}S_{\uparrow}}}{A^I_{P_{\downarrow}}} \\
&\quad -\frac{C^{II}_T}{C^I_T}\frac{k^2_{c1}-k^2_{zp1}}{2k_{c1}(k_{c2}+k_{zp2})}\frac{A^{II}_{P_{\downarrow}P_{\downarrow}}}{A^I_{P_{\downarrow}}} - \frac{C^{II}_T}{C^I_T}\frac{k^2_{c1}-k^2_{zp1}}{2k_{c1}(k_{c2}+k_{zs2})}\frac{A^{II}_{P_{\downarrow}S_{\downarrow}}}{A^I_{P_{\downarrow}}}.
\end{aligned}
$$

By expanding each individual term in the above equation up to the first order of $\Delta\alpha/\alpha$, $\Delta\beta/\beta$ and $\Delta\rho/\rho$, and making use of Chapman's result, we obtain

$$
\frac{P^R_{tube}}{P_{inc}} = R_\rho\frac{\Delta\rho}{\rho} + R_\beta\frac{\Delta\beta}{\beta} + R_\alpha\frac{\Delta\alpha}{\alpha} \qquad \text{(C-1)}
$$

where

$$
\begin{aligned}
R_\rho &= \frac{1}{2}\frac{K_-}{M}(\frac{1}{2} - R + \frac{K_+ - K_-}{4K_+}Q) + \frac{1}{2}\frac{K_+}{M}(\frac{1}{2} - 2\beta^2 p^2) \\
&\quad + \frac{1}{2}\frac{NK_-K_+}{M^2}\,[(1 - 2\beta^2 p^2 + 2\beta^2 \frac{\cos i}{\alpha}\frac{\cos j}{\beta}) \\
&\quad \frac{\beta^2 p^2\sqrt{1-\beta^2 p^2}}{J_- \cos j(1 - 2\beta^2/\alpha^2 + \beta^2 p^2)} - (1 - 2\beta^2 p^2 - 2\beta^2 \frac{\cos i}{\alpha}\frac{\cos j}{\beta})\frac{\beta p \sin j}{J_+}] \\
R_\beta &= \frac{K_-}{M}(\frac{1}{1 - 2\beta^2/\alpha^2 \cos^2 i} - R + \frac{K_+ - K_-}{4K_+}Q) - 2\frac{K_+}{M}\beta^2 p^2 \\
&\quad -2\frac{NK_-K_+}{M^2}\beta^2\,[(p^2 - \frac{\cos i}{\alpha}\frac{\cos j}{\beta})\frac{\beta^2 p^2\sqrt{1-\beta^2 p^2}}{J_- \cos j(1 - 2\beta^2/\alpha^2 + \beta^2 p^2)} \\
&\quad -(p^2 + \frac{\cos i}{\alpha}\frac{\cos j}{\beta})\frac{\beta p \sin j}{J_+}] \\
R_\alpha &= -\frac{1}{2}\frac{K_-}{M}(\frac{K_+ - K_-}{2K_+}\frac{1}{1 - \alpha^2 p^2} + \frac{\alpha^2 + 6\beta^2 \cos^2 i}{2\cos^2 i(\alpha^2 - 2\beta^2 \cos^2 i)}) + \frac{1}{2}\frac{K_+}{M}\frac{1}{2\cos^2 i}
\end{aligned}
$$

where

$$
\begin{gathered}
K_- = \alpha\sqrt{1 + \rho_f\alpha_f^2/\rho\beta^2} - \alpha_f\sqrt{1 - p^2\alpha^2} \\
K_+ = \alpha\sqrt{1 + \rho_f\alpha_f^2/\rho\beta^2} + \alpha_f\sqrt{1 - p^2\alpha^2} \\
J_- = \beta\sqrt{1 + \rho_f\alpha_f^2/\rho\beta^2} - \alpha_f\sqrt{1 - p^2\beta^2} \\
J_+ = \beta\sqrt{1 + \rho_f\alpha_f^2/\rho\beta^2} + \alpha_f\sqrt{1 - p^2\beta^2} \\
R = \rho_f\alpha_f^2/(\rho\beta^2 + \rho_f\alpha_f^2),\ Q = 1 - R \\
M = \alpha\sqrt{1 + \rho_f\alpha_f^2/\rho\beta^2},\ N = \beta\sqrt{1 + \rho_f\alpha_f^2/\rho\beta^2}.
\end{gathered}
$$

Appendix D. EQUIVALENCE CONDITIONS

In this appendix, we prove that, up to a constant factor, the pressure at the center of fluid generated by a plane P wave incidence is identical to that generated by a ring of point sources as long as the ring source is located at a great distance from the borehole and the aperture of the measurement is small.

For a particular point source at (r_0, ν, z_0), the source potential at (r, θ, z) can be written as

$$\phi_{point} = \frac{e^{ik_\alpha R}}{R} = \frac{i\pi}{2\pi} \int_{-\infty}^{\infty} H_0^{(1)}(k_r \bar{r}) e^{ik_z(z-z_0)} dk_z \tag{D-1}$$

where $R = \sqrt{r^2 + r_0^2 - 2rr_0\cos(\theta - \nu) + (z - z_0)^2}$, $\bar{r} = \sqrt{r^2 + r_0^2 - 2rr_0\cos(\theta - \nu)}$ and $k_r = \sqrt{k_\alpha^2 - k_z^2}$.

Following Morse and Feshbach (1953), we have

$$\phi_{point} = \frac{i\pi}{2\pi} \int_{-\infty}^{\infty} [J_0(k_r r) H_0^{(1)}(k_r r_0) + 2 \sum_{n=1}^{\infty} J_n(k_r r) H_n^{(1)}(k_r r_0) \cos n(\theta - \nu)] \, e^{ik_z(z-z_0)} dk_z.$$

The potential of a ring of point sources is the integral of (D-1) with respect to ν, i.e.,

$$\phi_{ring} = \int_0^{2\pi} \phi_{point} d\nu = i\pi \int_{-\infty}^{\infty} J_0(k_r r) H_0^{(1)}(k_r r_0) e^{ik_z(z-z_0)} dk_z.$$

If the ring source is far away from the observation point, we can make use of the following asymptotic expansion

$$H_0^{(1)}(k_r r_0) = \sqrt{\frac{2}{\pi k_r r_0}} \, e^{i(k_r r_0 - \frac{\pi}{4})}$$

so the ring source potential is

$$\phi_{ring} = i\pi \sqrt{\frac{2}{\pi r_0}} \, e^{-i\frac{\pi}{4}} \int_{-\infty}^{\infty} \frac{J_0(k_r r)}{\sqrt{k_r}} \, e^{ik_r r_0 + ik_z(z-z_0)} dk_z.$$

As $r_0 \to \infty$, the stationary phase method is used to evaluate the integral. The stationary point is at

$$\frac{\partial f(k_z)}{\partial k_z} = 0 \tag{D-2}$$

where $f(k_z) = \sqrt{k_\alpha^2 - k_z^2}\, r_0 + k_z (z - z_0)$.

The solution to (D-2) is

$$k_z = k_\alpha \cos\delta$$

where $\cos\delta = (z - z_0)/\sqrt{r_0^2 + (z - z_0)^2}$ is a constant if the measurement aperture is small.

The ring source potential then can be reduced to

$$\phi_{ring} = A(r_0, z_0)\, J_0(k_\alpha \sin\delta\, r)\, \exp(ik_\alpha \cos\delta\, z) \tag{D-3}$$

where the constant A is given by

$$A(r_0, z_0) = 2i\pi r_0^{-\frac{1}{2}} e^{-i\frac{\pi}{4}} \sin\delta\, \exp(ik_\alpha \sin\delta\, r_0 - ik_\alpha \cos\delta\, z_0).$$

The displacement potential for an incident plane P wave is (Schoenberg, 1986)

$$\begin{aligned}\phi_P &= \exp(ik_\alpha \sin\delta\, r\cos(\theta - \nu) + ik_\alpha \cos\delta\, z) \\ &= \exp(ik_\alpha \cos\delta\, z)\,[J_0(k_\alpha \sin\delta\, r) + 2\sum_{n=1}^{\infty} i^n J_n(k_\alpha \sin\delta\, r)\cos n(\theta - \nu)]\end{aligned}$$

where ν is the azimuth of incident plane wave and δ is the incidence angle.

All modes except $n = 0$ will contribute zero pressure at the center of fluid. For the pressure at $r = 0$, the equivalent source potential will be

$$\phi_P^{eq} = J_0(k_\alpha \sin\delta\, r)\, \exp(ik_\alpha \cos\delta\, z). \tag{D-4}$$

Therefore, we arrive at our conclusion that

$$\phi_{ring}(r, z) = A(r_0, z_0)\, \phi_P^{eq}(r, z).$$

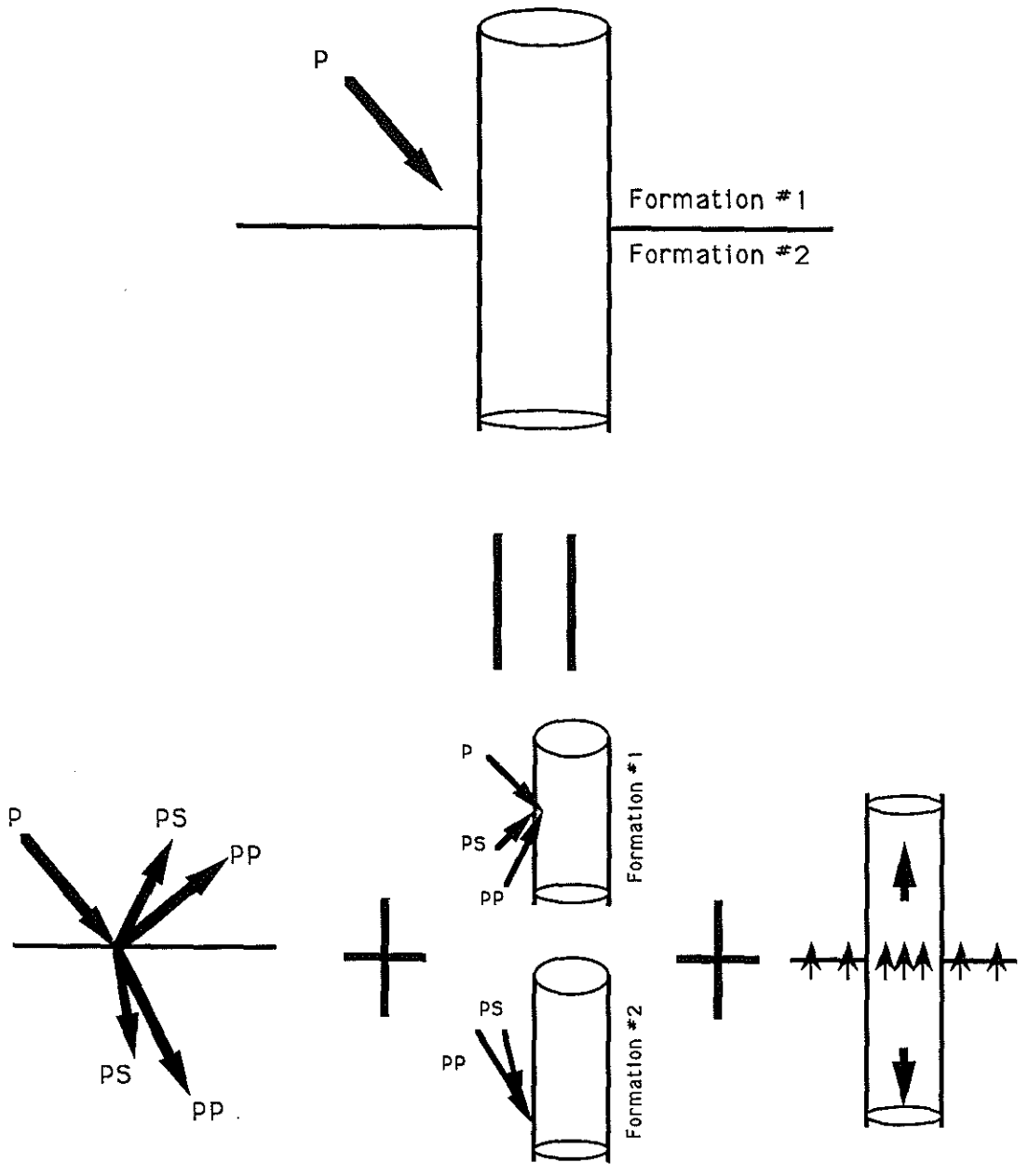

Figure 1: Tube wave generation at a layer boundary for an incident compressional plane wave and decomposition of the problem into three small problems.

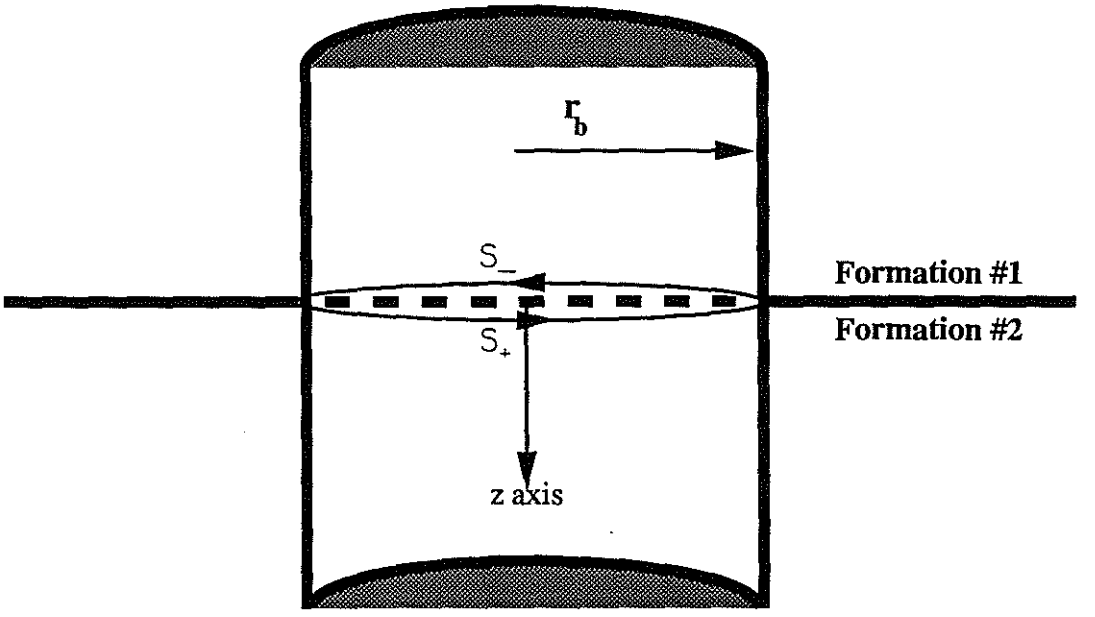

Elastic Representation Theory:

The elastic displacement can be expressed in terms of a surface integral of dislacement and traction discontinuity across the surface.

Figure 2: Cartoon showing the elastic representation theory.

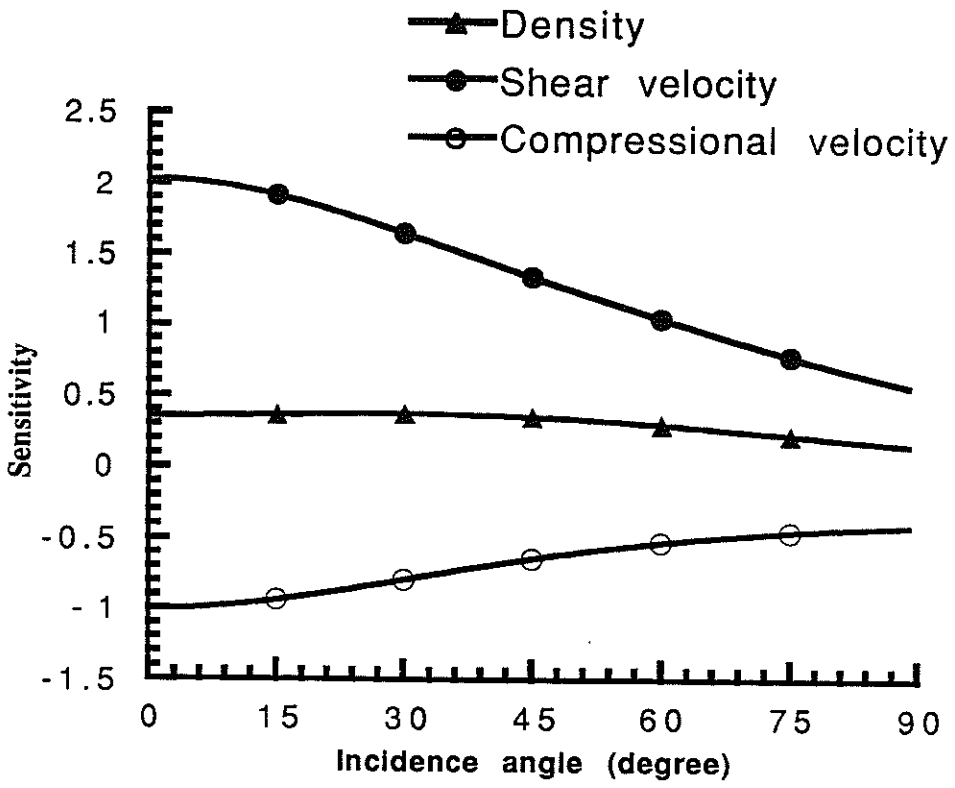

Figure 3: Sensitivity to the formation elastic parameters of the ratio of amplitude of the reflected tube wave to that of incident compressional wave as a function of incident angle.

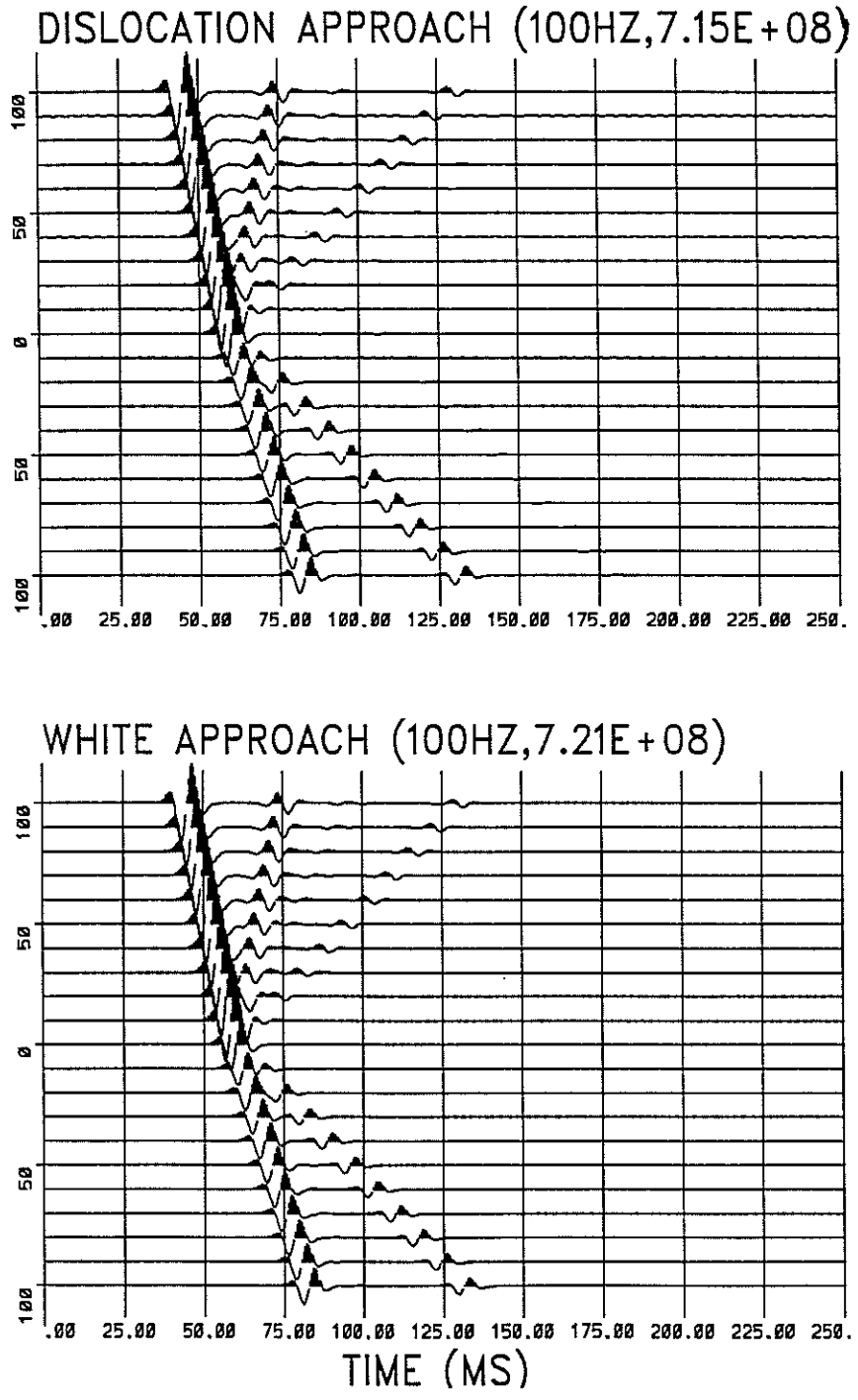

Figure 4: In this example, $\alpha_1 = 5970\, m/s$, $\beta_1 = 2880\, m/s$, $\rho_1 = 2656\, Kg/m^3$ and $\alpha_2 = 4206\, m/s$, $\beta_2 = 2664\, m/s$, $\rho_2 = 2140\, Kg/m^3$ and frequency 100 Hz, incident angle 25°.

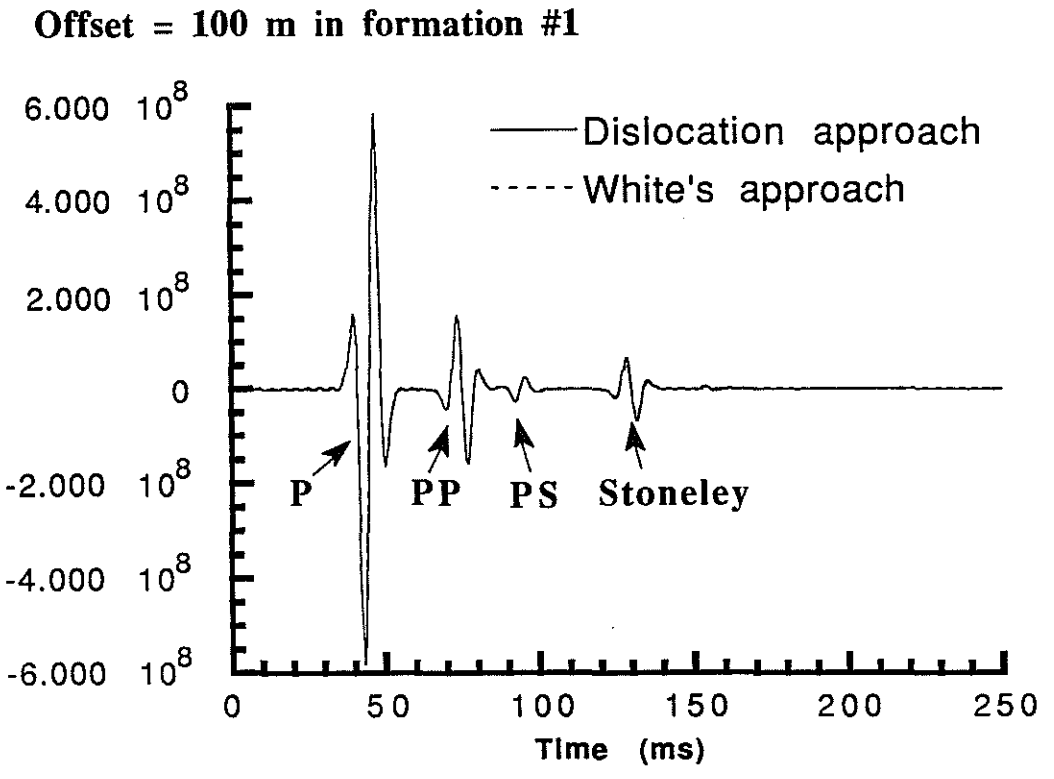

Figure 5: Overlay of the first trace in both plots of Figure 4.

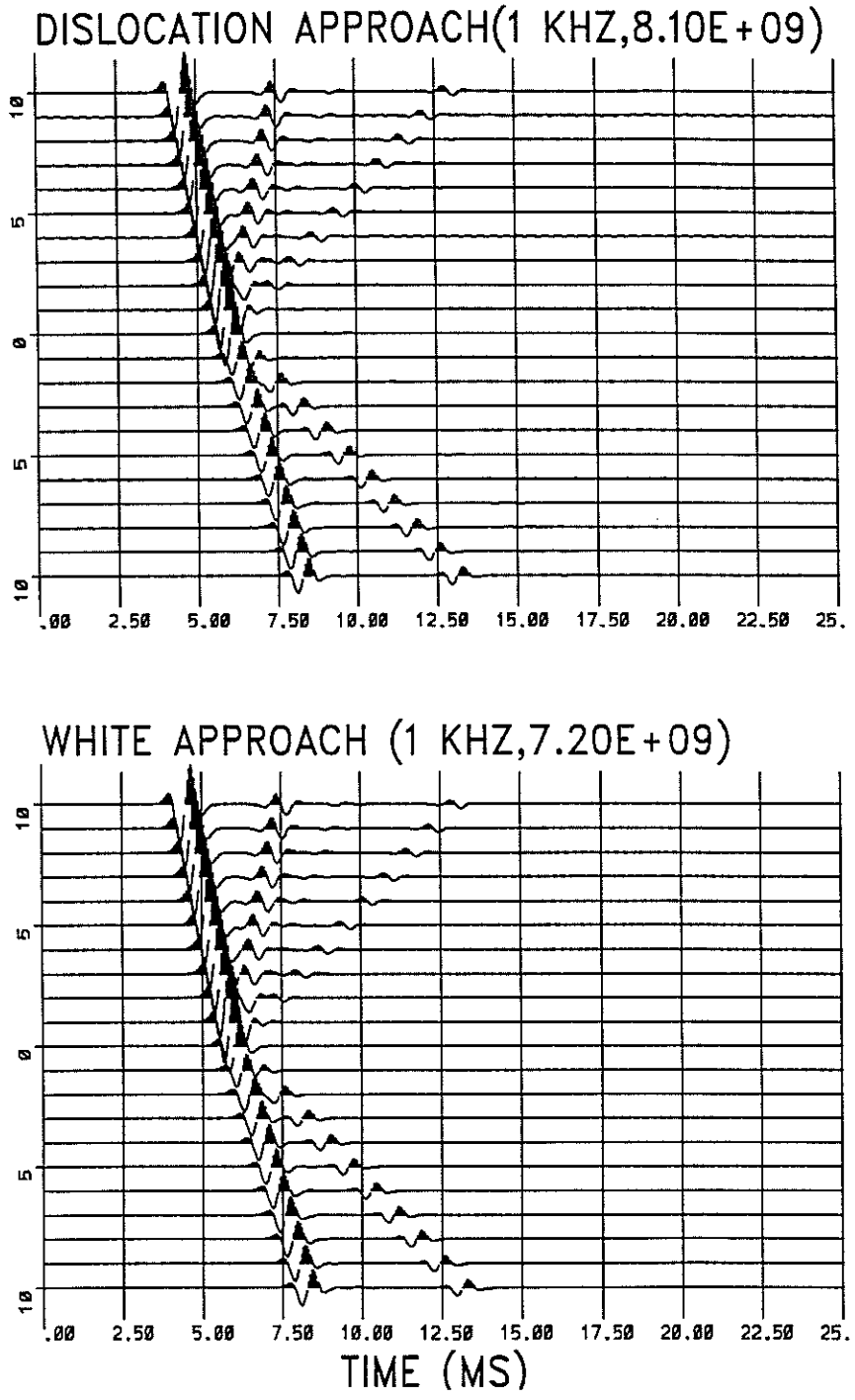

Figure 6: Same as Figure 4 except 1000 Hz.

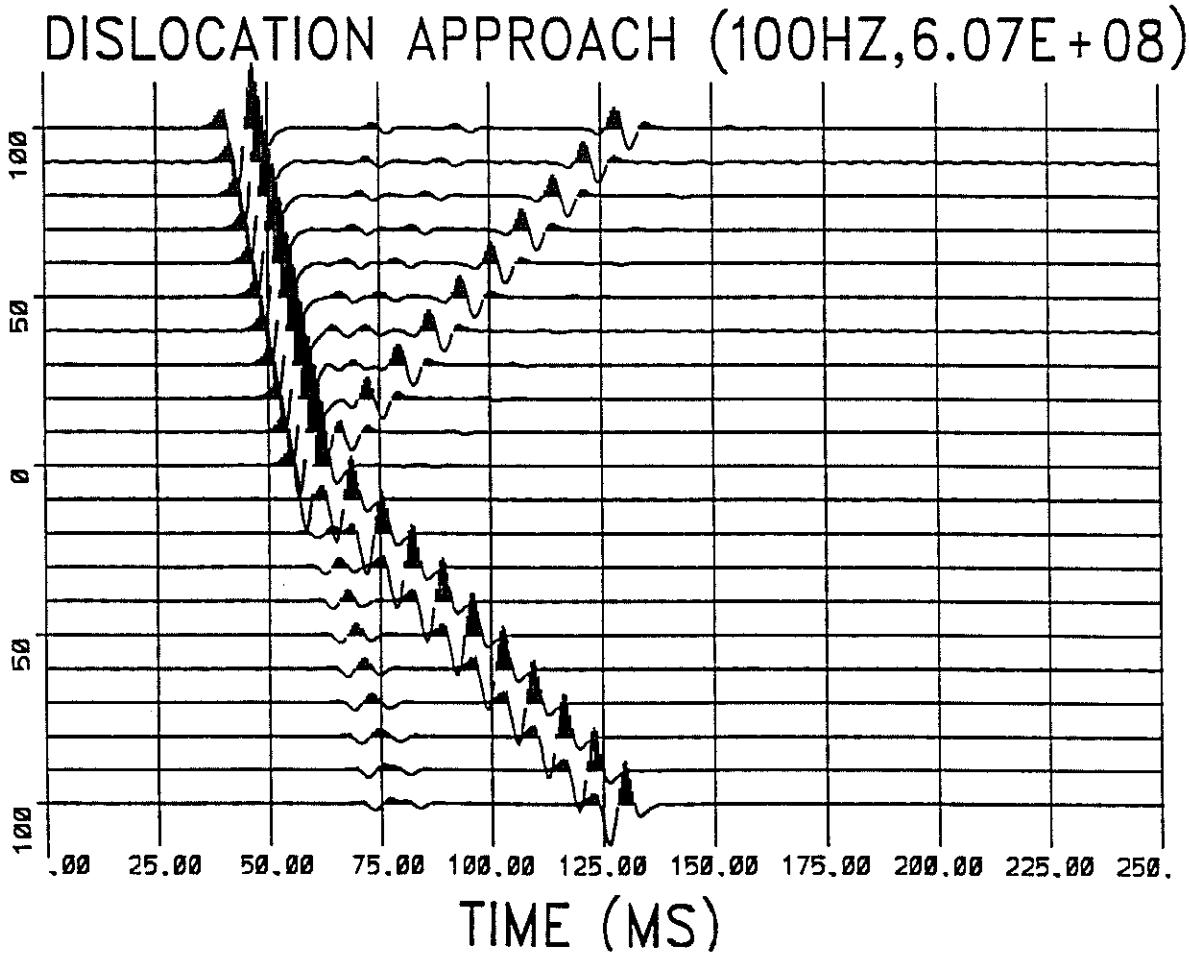

Figure 7: In this example, $\alpha_1 = 5970\, m/s$, $\beta_1 = 2880\, m/s$, $\rho_1 = 2656\, Kg/m^3$ and $\alpha_2 = 5970\, m/s$, $\beta_2 = 4320\, m/s$, $\rho_2 = 2656\, Kg/m^3$ and frequency 100 Hz, incident angle 25°.

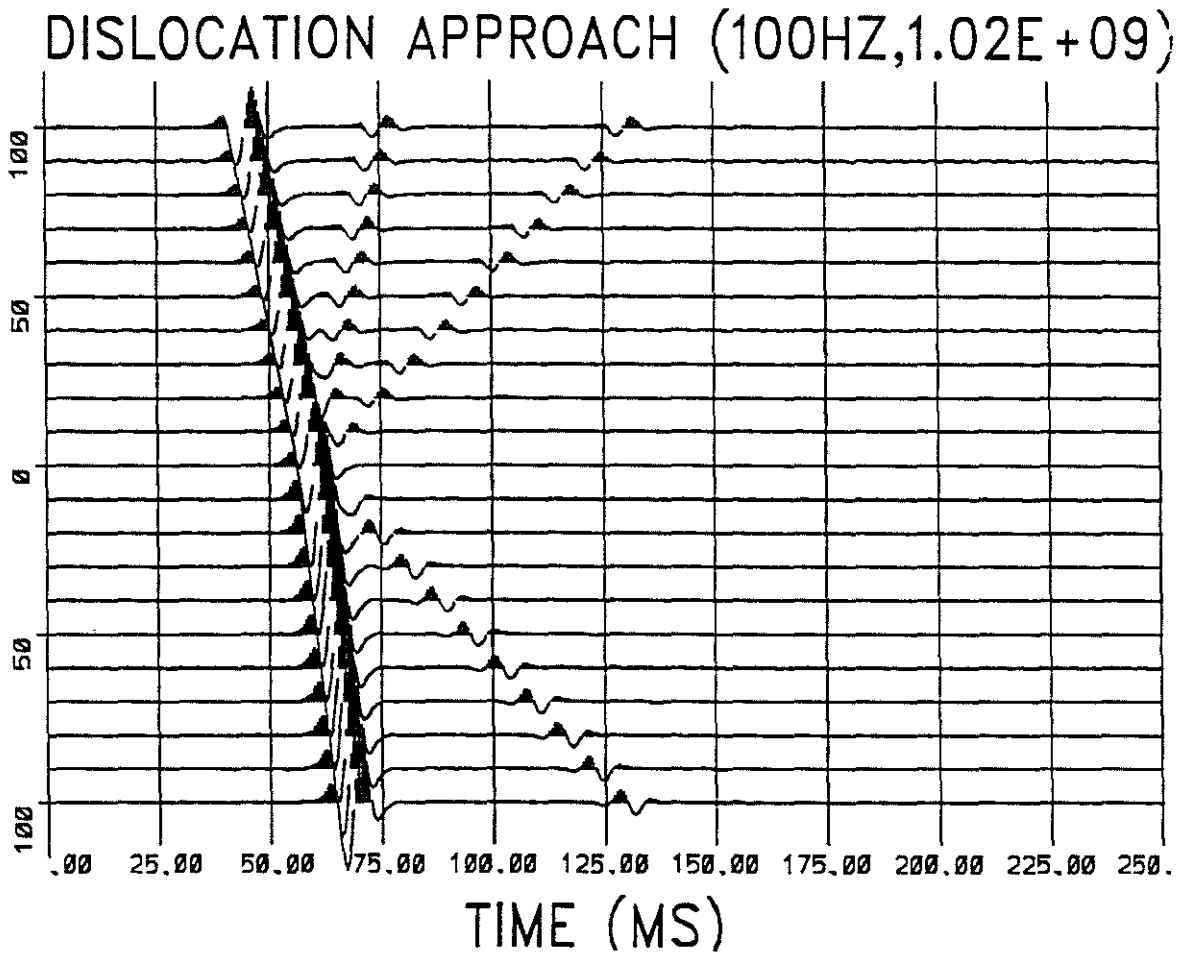

Figure 8: In this example, $\alpha_1 = 5970\, m/s$, $\beta_1 = 2880\, m/s$, $\rho_1 = 2656\, Kg/m^3$ and $\alpha_2 = 8955\, m/s$, $\beta_2 = 2880\, m/s$, $\rho_2 = 2656\, Kg/m^3$ and frequency 100 Hz, incident angle 25^o.

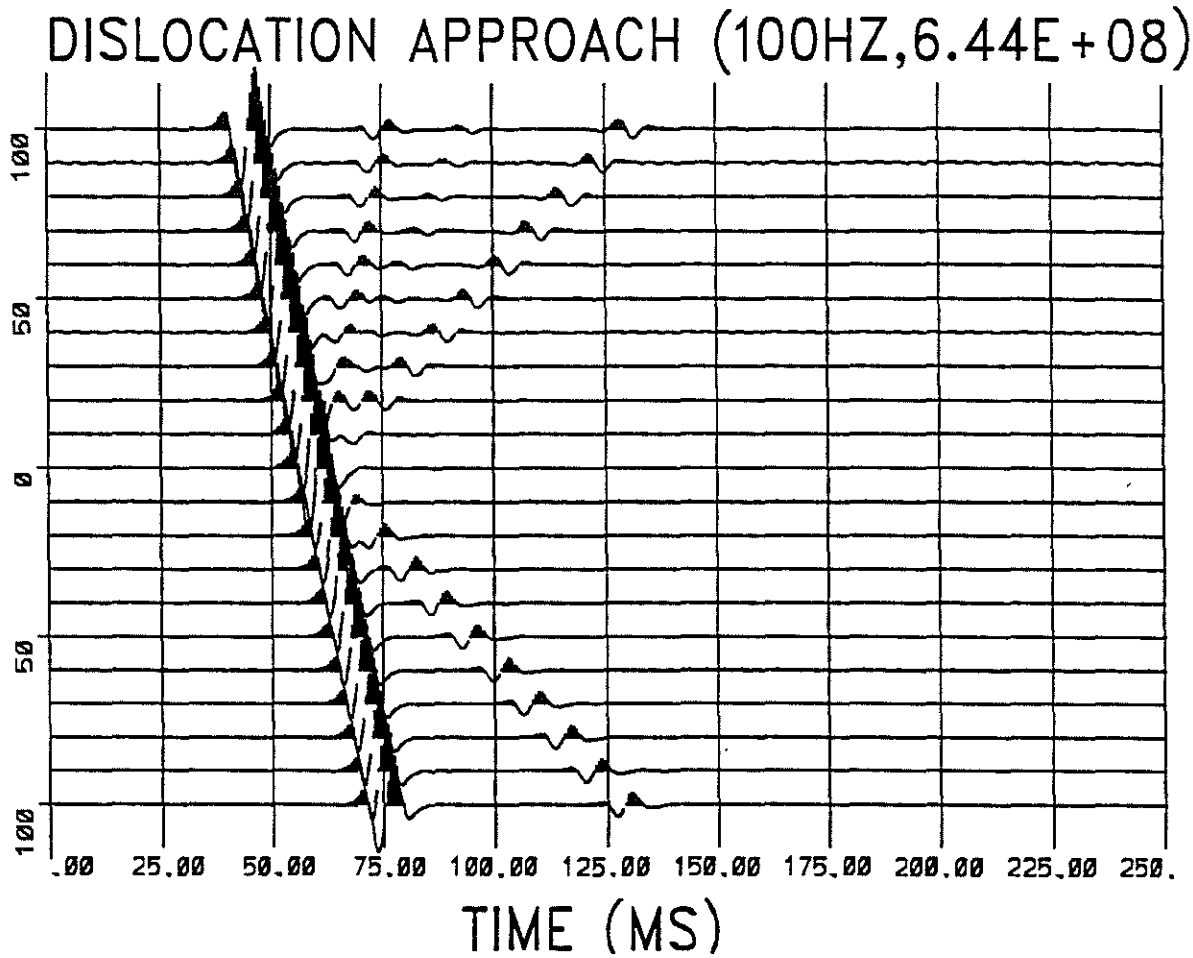

Figure 9: In this example, $\alpha_1 = 5970\, m/s$, $\beta_1 = 2880\, m/s$, $\rho_1 = 2656\, Kg/m^3$ and $\alpha_2 = 5970\, m/s$, $\beta_2 = 2880\, m/s$, $\rho_2 = 3984\, Kg/m^3$ and frequency 100 Hz, incident angle 25^o.

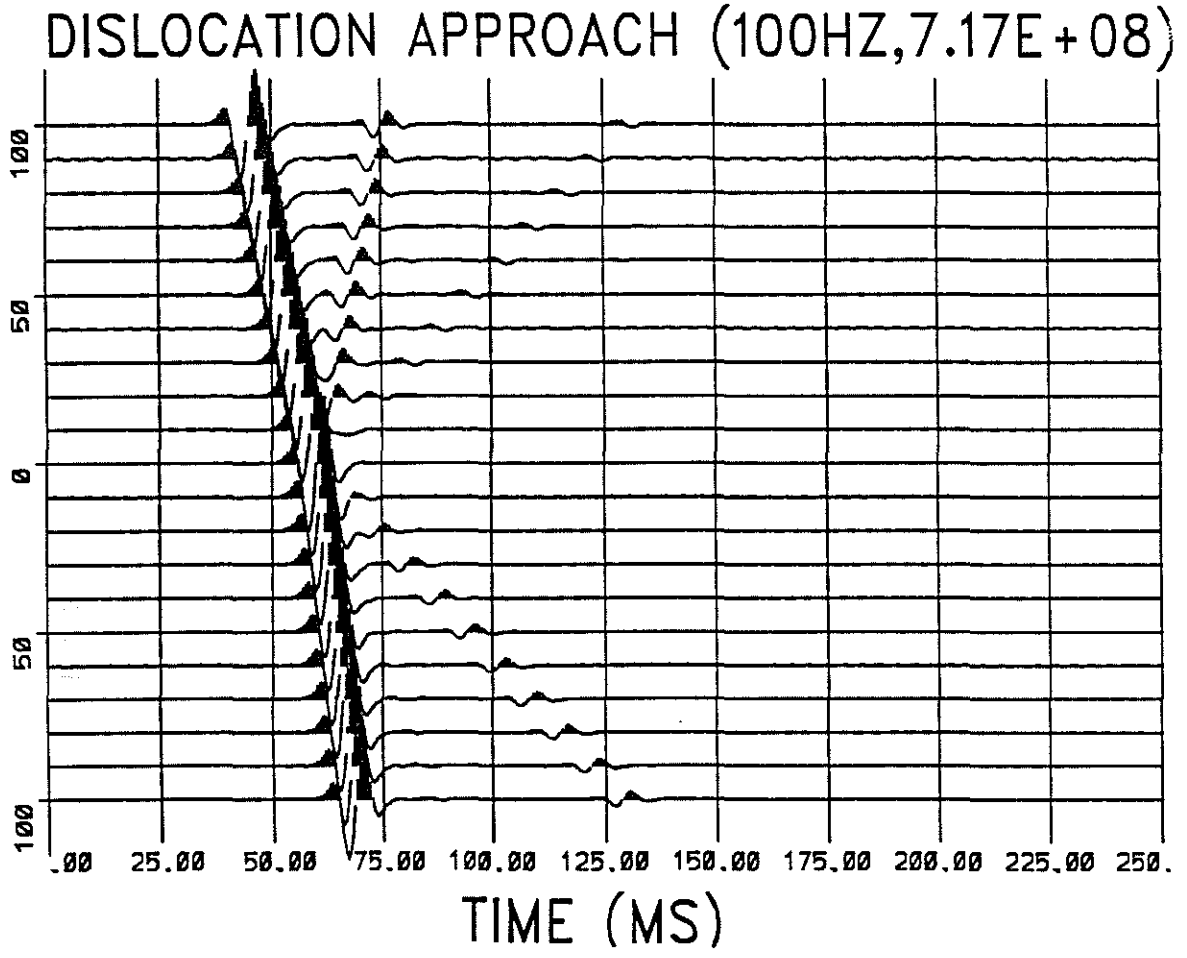

Figure 10: In this example, $\alpha_1 = 5970\, m/s$, $\beta_1 = 2880\, m/s$, $\rho_1 = 2656\, Kg/m^3$ and $\alpha_2 = 8955\, m/s$, $\beta_2 = 3600\, m/s$, $\rho_2 = 2656\, Kg/m^3$ and frequency 100 Hz, incident angle 25^o.

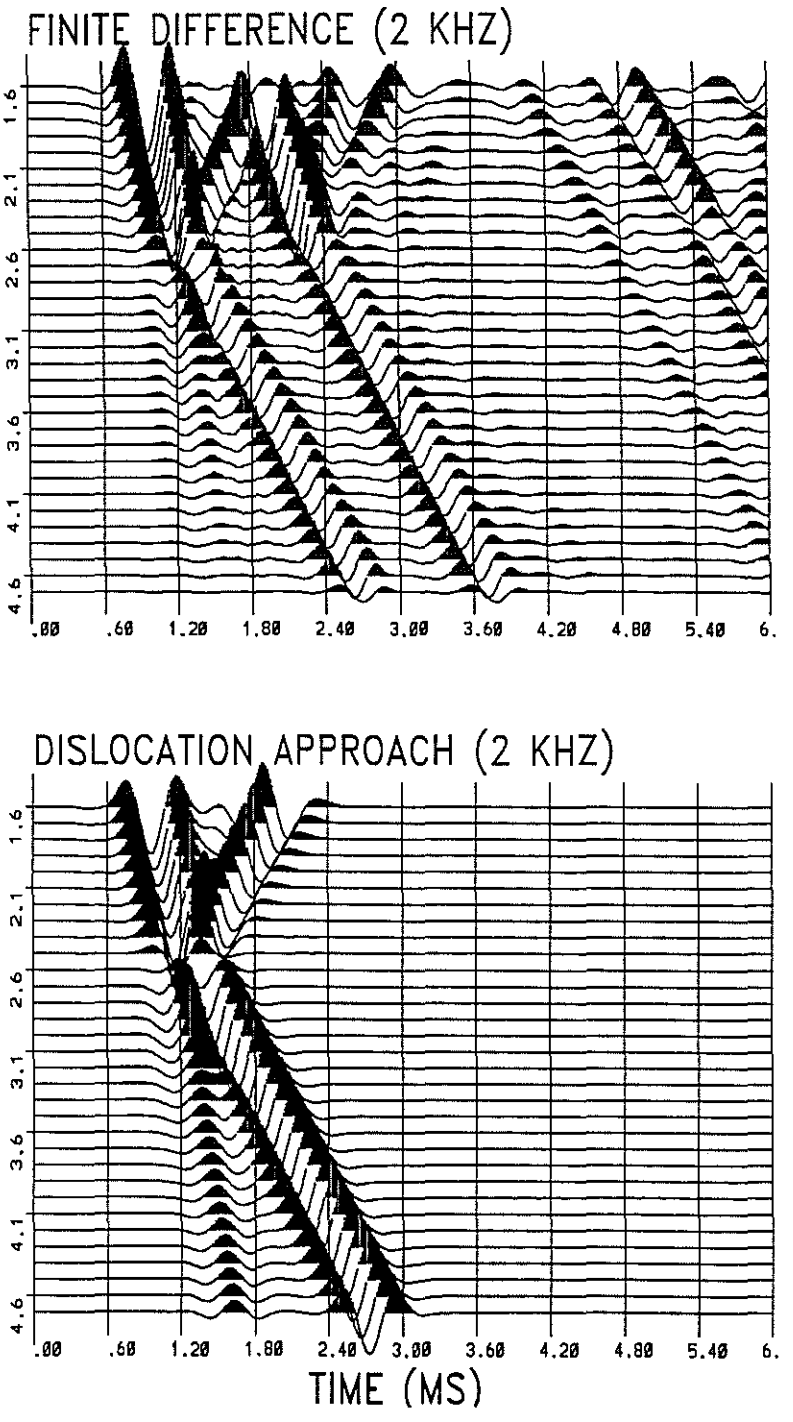

Figure 11: In this example, $\alpha_1 = 2700\, m/s$, $\beta_1 = 1400\, m/s$, $\rho_1 = 2000\, Kg/m^3$ and $\alpha_2 = 6300\, m/s$, $\beta_2 = 3400\, m/s$, $\rho_2 = 2700\, Kg/m^3$ and frequency 2000 Hz. (a) Finite difference calculation for a ring source at 2 m inside the formation and (b) negative dislocation approach for an plane P wave at incident angle 37°.